

ADMM Algorithms for Residual Network Training: Convergence Analysis and Parallel Implementation

Jintao Xu*, Yifei Li, Wenzhong Xing

Abstract—We propose both serial and parallel proximal (linearized) alternating direction method of multipliers (ADMM) algorithms for training residual neural networks. In contrast to backpropagation-based approaches, our methods inherently mitigate the exploding gradient issue and are well-suited for parallel and distributed training through regional updates. Theoretically, we prove that the proposed algorithms converge at an R-linear (sublinear) rate for both the iteration points and the objective function values. These results hold without imposing stringent constraints on network width, depth, or training data size. Furthermore, we theoretically analyze our parallel/distributed ADMM algorithms, highlighting their reduced time complexity and lower per-node memory consumption. To facilitate practical deployment, we develop a control protocol for parallel ADMM implementation using Python’s multiprocessing and interprocess communication. Experimental results validate the proposed ADMM algorithms, demonstrating rapid and stable convergence, improved performance, and high computational efficiency. Finally, we highlight the improved scalability and efficiency achieved by our parallel ADMM training strategy.

Index Terms—Residual neural networks, alternating direction method of multipliers (ADMM), convergence analysis, parallel training.

I. INTRODUCTION

THE residual learning framework and its corresponding residual neural network architecture were originally proposed to facilitate effective training of deep neural networks (DNNs) for image recognition tasks [1]. Since their inception, these techniques have rapidly become foundational paradigms within DNN design. In particular, residual connections continue to play a pivotal role in state-of-the-art deep learning applications, including large language models (LLMs). For example, residual connections are integral components of both the encoder and decoder structures in the transformer model [2], which underpins leading LLMs such as BERT [3] and the GPT series [4], [5].

Jintao Xu is with Department of Applied Mathematics, The Hong Kong Polytechnic University, Hong Kong, China. (jintao.xu@polyu.edu.hk)

Yifei Li is an independent scholar. Yifei Li is currently affiliated with Alibaba Group. This work is not associated with Alibaba Group and does not reflect the views of the company. (liyifei.411@outlook.com)

Wenzhong Xing is with Department of Mathematical Sciences, Tsinghua University, Beijing 100084, China. (wxing@mail.tsinghua.edu.cn)

Corresponding author: Jintao Xu

This work was supported in part by the National Natural Science Foundation of China Grant No. 11771243, PolyU postdoc matching fund scheme of The Hong Kong Polytechnic University Grant No. 1-W35A, and Huawei’s Collaborative Grants “Large scale linear programming solver” and “Solving large scale linear programming models for production planning”.

The expression $h(\mathbf{x}) + \varphi(\mathbf{x})$ is termed a residual connection or residual block in neural network architectures, where $\mathbf{x} \in \mathbb{R}^n$, and $h, \varphi : \mathbb{R}^n \rightarrow \mathbb{R}^m$. Typically, $m = n$, and h is chosen as the identity mapping. The selection of φ determines the specific type of residual network, for instance, conventional residual networks rely on standard convolutional operations [1], whereas transformer-based architectures incorporate multi-head attention mechanisms [2].

Neural network training remains a core research topic, attracting attention in both deep learning and optimization communities [6]–[13]. In this paper, we address the following *multi-block nonconvex* optimization problem for training an N -layer residual network:

$$\min_{\mathbf{W}} \frac{1}{n} \sum_{j=1}^n \ell(\mathbf{v}_N(\mathbf{x}_j; \mathbf{W}), \mathbf{y}_j) + \lambda \Omega(\mathbf{W}) \quad (1)$$

where $\mathbf{W} := (\text{vec}(\mathbf{W}_1), \dots, \text{vec}(\mathbf{W}_N))$, the i th layer contains d_i neurons, $\varphi_i(\mathbf{x}) := \sigma_i(\mathbf{W}_i \mathbf{v})$ with the element-wise activation function $\sigma_i : \mathbb{R} \rightarrow \mathbb{R}$ for each $i \in [N]^1$, the output vectors $\mathbf{v}_N(\mathbf{x}_j; \mathbf{W}) = f_N \circ \dots \circ f_1(\mathbf{x}_j)$ with $f_i(\mathbf{x}) := h_i(\mathbf{x}) + \varphi_i(\mathbf{x})$ for $i \in [N-1]$ and $f_N(\mathbf{x}) := \mathbf{W}_N \mathbf{x}$ for each $j \in [n]$, $\{(\mathbf{x}_j, \mathbf{y}_j)\}_{j=1}^n \subseteq \mathbb{R}^{d_0} \times \mathbb{R}^{d_N}$ are the given n pairs of training data, $\ell : \mathbb{R}^{d_N} \times \mathbb{R}^{d_N} \rightarrow \mathbb{R}_+$ denotes the loss function, $\Omega : \mathbb{R}^d \rightarrow \mathbb{R}$ denotes the regularization with $d := \sum_{i=0}^{N-1} d_i d_{i+1}$, and parameter $\lambda > 0$.

Backpropagation-based (BP-based) algorithms, including stochastic gradient descent (SGD), SGD with momentum (SGDM), and Adam [14], are widely used to train neural networks. They calculate gradients by iteratively propagating partial derivatives throughout the network using the chain rule. However, as highlighted in [6], [15], [16], BP-based algorithms present several notable limitations, described as follows.

- 1) When computing gradients through the chain rule, BP-based training algorithms encounter the well-known exploding gradient issue during the training of DNNs [17]. This phenomenon causes the magnitude of (stochastic) gradient components to progressively increase, thereby hindering effective training and potentially leading to computational failures (see Section VII).
- 2) To update the weight matrix in the i th layer, partial-derivatives with respect to all preceding layers (i.e., layers $i-1$ through 1) must first be computed. Due to the inherently sequential nature of this gradient computation, BP-based training methods do not readily lend themselves to parallelization across layers [18].

¹For simplicity, we omit the bias term.

3) In distributed training scenarios, the scalability of BP-based methods is inherently limited. Specifically, the sequential dependency induced by the chain rule restricts layer-wise partitioning across multiple computational nodes. Consequently, each node typically maintains a complete copy of the network weights, leading to significant memory and storage overhead.

The alternating direction method of multipliers (ADMM) [19] is a widely adopted optimization technique that updates primal variables by solving subproblems derived from the augmented Lagrangian, followed by dual variable updates in each iteration. To address the limitations inherent to BP-based methods, we propose a family of serial and parallel ADMM-based training algorithms specifically designed for residual neural networks, herein referred to as **RADMM**. Our approach leverages the structural properties of residual networks, thereby effectively circumventing the sequential dependencies imposed by the chain rule. *Consequently, the proposed RADMM framework mitigates the above drawbacks of BP-based training as below.*

- 1) By eliminating gradient computations based on the chain rule, the proposed approach effectively addresses the exploding gradient issues commonly encountered in BP-based methods.
- 2) By leveraging the proposed parallel regional update (**PRU**) strategy, our algorithms naturally facilitate parallel execution across network layers (see Section VI-A), significantly reducing computational time.
- 3) By enabling each computing node to store only the variables associated with its corresponding block, our proposed approach significantly reduces per-node memory requirements during distributed training.

To facilitate the development of parallelizable proximal (linearized) RADMM algorithms (see Definition 1 for the proximal (linearized) operator), we first reformulate problem (1) into an equivalent constraint multi-block nonconvex optimization formulation that fully exploits the inherent structural properties of residual networks, as follows.

$$\begin{aligned} \min_{\mathbf{W}} \mathcal{J} &:= \frac{1}{n} \sum_{j=1}^n \ell(\mathbf{v}_N^j, \mathbf{y}_j) + \lambda \Omega(\mathbf{W}) \\ \text{s.t. } \mathbf{v}_i^j &= h_i(\mathbf{v}_{i-1}^j) + \sigma_i \circ g_i(\mathbf{v}_{i-1}^j; \mathbf{W}_i), i \in [N-1], j \in [n], \\ \mathbf{v}_N^j &= \mathbf{W}_N \mathbf{v}_{N-1}^j, j \in [n], \end{aligned} \quad (2)$$

where $\mathbf{v}_0^j = \mathbf{x}_j$ for each $j \in [n]$, and $\mathbf{W}_i, i = 1, \dots, N$ are tightly coupled, significantly hindering efficient and parallel training of residual networks.

By introducing a set of auxiliary decision variables $\{\mathbf{v}_i^j\}$, we derive the following relaxation model termed the two-splitting relaxation, which forms the basis for designing two-splitting proximal (linearized) RADMMs (see Section IV):

$$\begin{aligned} \min_{\mathbf{W}, \mathbf{v}} \mathcal{J} &+ \frac{\mu}{2} \sum_{j=1}^n \sum_{i=1}^{N-1} \|h_i(\mathbf{v}_{i-1}^j) + \sigma_i \circ g_i(\mathbf{v}_{i-1}^j; \mathbf{W}_i) - \mathbf{v}_i^j\|^2 \\ \text{s.t. } \mathbf{v}_N^j &= \mathbf{W}_N \mathbf{v}_{N-1}^j, j \in [n], \end{aligned} \quad (3)$$

where $\mathbf{v} := (\mathbf{v}_i^j)$, and $\mu > 0$. Furthermore, to improve training efficiency of deeper residual networks, as suggested in [20], we introduce an additional set of auxiliary decision variables $\{\mathbf{u}_i^j\}$. Consequently, the network can be reformulated as:

$$\begin{aligned} \mathbf{v}_i^j &= h_i(\mathbf{v}_{i-1}^j) + \sigma_i(\mathbf{u}_i^j); \\ \mathbf{u}_i^j &= g_i(\mathbf{v}_{i-1}^j; \mathbf{W}_i), i \in [N-1], j \in [n]. \end{aligned}$$

Then we derive the following relaxation, termed the three-splitting relaxation, which serves as the foundation for developing the three-splitting proximal (linearized) RADMM algorithms (see Section V):

$$\begin{aligned} \min_{\mathbf{W}, \mathbf{u}, \mathbf{v}} \mathcal{J} &+ \frac{\mu}{2} \sum_{j=1}^n \sum_{i=1}^{N-1} \|h_i(\mathbf{v}_{i-1}^j) + \sigma_i(\mathbf{u}_i^j) - \mathbf{v}_i^j\|^2 \\ \text{s.t. } \mathbf{u}_i^j &= g_i(\mathbf{v}_{i-1}^j; \mathbf{W}_i), i \in [N-1], j \in [n], \\ \mathbf{v}_N^j &= \mathbf{W}_N \mathbf{v}_{N-1}^j, j \in [n], \end{aligned} \quad (4)$$

where $\mathbf{u} := (\mathbf{u}_i^j)$.

For simplicity, we adopt the mean squared error (MSE) loss for ℓ , employ the ridge regression penalty for Ω , and set h_i as the identity mapping. Accordingly, problem (2) can be reformulated as the following matrix optimization problem:

$$\begin{aligned} \min_{\mathbf{W}} \mathcal{J}(\mathbf{W}, \mathbf{V}_N) &:= \frac{1}{2} \|\mathbf{V}_N - \mathbf{Y}\|^2 + \frac{\lambda}{2} \sum_{i=1}^N \|\mathbf{W}_i\|^2 \\ \text{s.t. } \mathbf{V}_i &= \mathbf{V}_{i-1} + \sigma_i(\mathbf{W}_i \mathbf{V}_{i-1}), i \in [N-1], \\ \mathbf{V}_N &= \mathbf{W}_N \mathbf{V}_{N-1}, \end{aligned} \quad (5)$$

where $\mathbf{X} := (\mathbf{x}_1, \dots, \mathbf{x}_n) \in \mathbb{R}^{d_0 \times n}$, $\mathbf{Y} := (\mathbf{y}_1, \dots, \mathbf{y}_n) \in \mathbb{R}^{d_N \times n}$, $\mathbf{V}_i := (\mathbf{v}_i^1, \dots, \mathbf{v}_i^n) \in \mathbb{R}^{d_0 \times n}$, $i \in [N-1]$ and $\mathbf{V}_N := (\mathbf{v}_N^1, \dots, \mathbf{v}_N^n) \in \mathbb{R}^{d_N \times n}$ are the output/input matrices of each layer. It should be noted that (5) is also a multi-block nonconvex optimization problem. As discussed in Section IV-B and Section V-B, the theoretical analysis of the convergence of RADMMs is challenging. Figure 1 illustrates the relationships among the training problem, the relaxation models, and the proximal (linearized) RADMM algorithms.

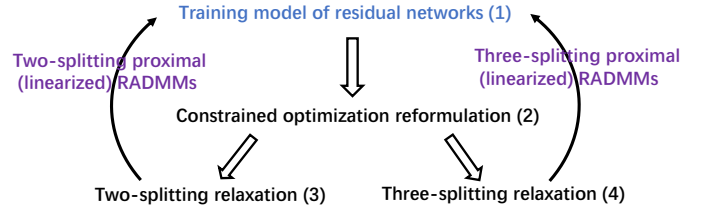


Fig. 1. Relationships between training problem, relaxations, and RADMMs.

The main contributions of this paper are summarized as below.

- 1) Algorithmically, we develop parallelizable proximal (linearized) ADMM training methods for residual networks (RADMMs) by exploiting their intrinsic structure, and incorporating auxiliary variables. Moreover, we implement our methods in parallel and distributed architectures via the Parallel Regional Update (PRU) approach.
- 2) Theoretically, we establish the convergence of both the iteration points and objective function values for the proposed serial and parallel proximal RADMM algorithms, without imposing restrictive assumptions on network width, depth, or dataset size. Furthermore, we prove that these algorithms exhibit an R-linear/sublinear convergence rate based on the value of the KL exponent.
- 3) Theoretically, we demonstrate that the proposed parallel strategy significantly reduces time complexity under conditions of low communication overhead. Additionally,

our distributed approach reduces the per-node runtime memory requirement from cubic to quadratic.

4) Empirically, the proposed RADMM algorithms exhibit faster and more stable convergence, improved performance, and higher training speed compared to SGD, SGDM, and Adam. Furthermore, we have developed and implemented a control protocol for parallel RADMM training using Python's multiprocessing and interprocess communication (IPC) mechanisms, demonstrating substantial advantages derived from parallelization.

The remainder of this paper is organized as follows. We start with the related work in Section II. Notations and definitions are shown in Section III. Next, two- and three-splitting RADMMs and their convergence analysis are presented in Section IV and Section V, respectively. Parallel, distributed algorithms and their advantages are shown in Section VI. Experiments are reported in Section VII. Finally, we make some concluding remarks in Section VIII.

II. RELATED WORK

A. Alternatives to BP-Based Training Algorithms

Algorithmically, Taylor et al. [6], Zeng et al. [10], Wang et al. [21], and Wang et al. [22] developed ADMM training algorithms for feedforward neural networks (FNNs). Moreover, this approach has been applied to train graph-augmented multilayer perceptrons [13]. Gu et al. [16] introduced a class of lifted relaxation models known as Fenchel lifted network. Li et al. [11] proposed the lifted proximal operator machine for FNN training. Li et al. [11], Gu et al. [16], and Zeng et al. [20] developed block coordinate descent (BCD) training algorithms for FNNs. Cui et al. [8] designed a majorization-minimization algorithm for an exact reformulation of the DNN training optimization problem. Liu et al. [12], [23] developed a smoothing proximal gradient algorithm and an inexact augmented Lagrangian algorithm for autoencoders and leaky ReLU DNNs with group sparsity training, respectively.

Theoretically, Cui et al. [8] demonstrated that any accumulation point of the sequence generated by the majorization-minimization training algorithm is a directional-stationary point. For the autoencoders training problem and related models, Liu et al. [12] investigated the relationships between global (or local) minimizers and (generalized) directional-stationary points. Moreover, for leaky ReLU DNNs with group sparsity training, Liu et al. [23] discussed the relationship between global (or local) minimizers and certain stationary points. Convergence of the BCD training algorithms is studied by [11], [20]. Zeng et al. [10] established both the convergence and an $\mathcal{O}(1/k)$ convergence rate for ADMM training algorithms applied to FNNs. Additionally, Xu et al. [24] provided a convergence rate analysis framework for a general class of alternating minimization-type DNNs training methods.

B. Alternating Direction Method of Multipliers

ADMM has attracted significant attention in the machine learning community [6], [10], [13], [21], [22], [25], [26]. It is well established that (proximal) ADMM converges for

two-block separable convex optimization problems subject to linear constraints [19], [27]. Moreover, by imposing additional assumptions, convergence results have been derived for the (semi-proximal) ADMM when applied to multi-block convex optimization problems with linear constraints [28], [29] as well as multi-block nonconvex optimization problems with linear constraints [30], [31].

C. DNNs Parallel Training

Parallel and distributed computing are widely employed in machine learning research. In the context of DNN training, two prevalent strategies are model parallelism and data parallelism [11], [13], [22], [32], [33]. With model parallelism, the neural network is partitioned into several segments, each trained on a separate processor. In contrast, data parallelism distributes subsets of the training data across processors, with each processor independently training the entire model using its local data.

III. PRELIMINARIES

A. Notations

$\|\cdot\|$ denotes the l_2 norm for vectors and the Frobenius norm for matrices, respectively. \odot denotes the Hadamard product, while $\underline{\lim} f$ denotes the limit inferior of f . \bar{v} and \underline{v} denote the upper and lower bounds of variable v , respectively. Additionally, $\text{vec}(\mathbf{X})$ denotes the vectorization of matrix \mathbf{X} . $\langle \mathbf{X}, \mathbf{Y} \rangle = \text{tr}(\mathbf{XY}^T)$ for matrices \mathbf{X} and \mathbf{Y} .

B. Optimization and Variational Analysis

Definition 1 ([34]). *Let f be a differentiable closed proper convex function. Then the mapping*

$$\text{prox}_{\frac{1}{\alpha}f}(\bar{\mathbf{x}}) = \arg \min_{\mathbf{x}} \left\{ f(\mathbf{x}) + \frac{\alpha}{2} \|\mathbf{x} - \bar{\mathbf{x}}\|^2 \right\}$$

with $\alpha > 0$, is said to be the proximal operator. And we also have the linearized version:

$$\arg \min_{\mathbf{x}} \left\{ \langle \nabla f(\bar{\mathbf{x}}), \mathbf{x} - \bar{\mathbf{x}} \rangle + \frac{\alpha}{2} \|\mathbf{x} - \bar{\mathbf{x}}\|^2 \right\}.$$

The history of Kurdyka-Łojasiewicz (KL) property goes back to the work of Kurdyka [35] and Łojasiewicz [36], [37]. We first present the next two definitions.

Definition 2 ([38], [39]). *The Fréchet subdifferential $\widehat{\partial}f(\mathbf{x})$ of f at $\mathbf{x} \in \text{dom}f$ is the following set*

$$\left\{ \mathbf{v} \left| \lim_{\mathbf{y} \rightarrow \mathbf{x}} \frac{f(\mathbf{y}) - f(\mathbf{x}) - \langle \mathbf{v}, \mathbf{y} - \mathbf{x} \rangle}{\|\mathbf{y} - \mathbf{x}\|} \geq 0 \right. \right\}.$$

Definition 3 ([38], [39]). *The limiting subdifferential $\partial f(\mathbf{x})$ of f at $\mathbf{x} \in \text{dom}f$ is the following set*

$$\{ \mathbf{v} \mid \exists \mathbf{x}^k \rightarrow \mathbf{x}, f(\mathbf{x}^k) \rightarrow f(\mathbf{x}), \mathbf{v}^k \rightarrow \mathbf{v}, \mathbf{v}^k \in \widehat{\partial}f(\mathbf{x}^k) \}.$$

Definition 4 ([34]). *A function f is called as proper if $f(\mathbf{x}) > -\infty$ for every \mathbf{x} and $f(\mathbf{x}) < \infty$ for at least one \mathbf{x} , and lower semicontinuous at \mathbf{x} if $f(\mathbf{x}) \leq \underline{\lim}_{k \rightarrow \infty} f(\mathbf{x}_k)$ for every sequence $\{\mathbf{x}_k\}$ satisfying $\mathbf{x}_k \rightarrow \mathbf{x}$.*

Definition 5 ([40], [41]). *A proper lower semicontinuous function f is said to have the Kurdyka-Łojasiewicz (KL) property at \mathbf{x}^* with exponent θ if there exist $c \in (0, +\infty)$, $\tau \in (0, +\infty]$, $\theta \in [0, 1]$ and an open set $\mathcal{N}_{\mathbf{x}^*}$ containing*

\mathbf{x}^* such that $(f(\mathbf{x}) - f(\mathbf{x}^*))^\theta \leq c \inf_{\mathbf{v} \in \partial f(\mathbf{x})} \|\mathbf{v}\|$ for all $\mathbf{x} \in \mathcal{N}_{\mathbf{x}^*} \cap \{\mathbf{x} | f(\mathbf{x}^*) < f(\mathbf{x}) < f(\mathbf{x}^*) + \tau\}$. Parameter θ is said to be KL exponent at \mathbf{x}^* .

Definition 6 ([42]). A function f , defined on an open set $\mathcal{U} \subseteq \mathbb{R}$, is called as real analytic on a subset $\mathcal{S} \subseteq \mathcal{U}$ if for every point $x \in \mathcal{S}$, there exists an interval $\mathcal{N}_x \subseteq \mathcal{U}$ centered at x such that $f(z) = \sum_{i=0}^{\infty} a_i(z - x)^i$ for all $z \in \mathcal{N}_x$.

In this paper, we assume that the activation σ_i for $i \in [N-1]$ are all real analytic such that there exist ψ_0 , ψ_1 , and ψ_2 satisfying $|\sigma_i(x)| \leq \psi_0$, $|\sigma'_i(x)| \leq \psi_1$, and $|\sigma''_i(x)| \leq \psi_2$. These assumptions are satisfied by the sigmoid, hyperbolic tangent, sine, and cosine functions. Notably, we do not impose any restrictions on the network depth $N \in \mathbb{N}_+$, the width $d_i \in \mathbb{N}_+$ of each layer, or the number n of samples.

IV. TWO-SPLITTING RADMMs

In this section, we introduce scalable two-splitting proximal (linearized) RADMM algorithms and provide their rigorous theoretical analysis.

A. Two-Splitting Proximal (Linearized) RADMMs

Our two-splitting RADMMs are designed based on the following constraint reformulation of (3) with MSE loss, ridge regression penalty, and identity mapping h_i , $i \in [N-1]$:

$$\begin{aligned} \min_{\mathbf{W}, \mathbf{V}} \quad & \mathcal{J}(\mathbf{W}, \mathbf{V}_N) + \frac{\mu}{2} \sum_{i=1}^{N-1} \|\mathbf{V}_{i-1} + \sigma_i(\mathbf{W}_i \mathbf{V}_{i-1}) - \mathbf{V}_i\|^2 \\ \text{s.t. } & \mathbf{V}_N = \mathbf{W}_N \mathbf{V}_{N-1}, \end{aligned} \quad (6)$$

where $\mathbf{V}_i = (\mathbf{v}_i^1, \dots, \mathbf{v}_i^n)$ for each $i \in [N]$, $\mathbf{V} := (\text{vec}(\mathbf{V}_1), \dots, \text{vec}(\mathbf{V}_N))$, and its augmented Lagrangian function:

$$\begin{aligned} \mathcal{L}_\beta^{2s}(\Psi_{2s}) := & \mathcal{J}(\mathbf{W}, \mathbf{V}_N) + \frac{\mu}{2} \sum_{i=1}^{N-1} \|\mathbf{V}_{i-1} + \sigma_i(\mathbf{W}_i \mathbf{V}_{i-1}) - \mathbf{V}_i\|^2 \\ & + \langle \mathbf{\Lambda}, \mathbf{W}_N \mathbf{V}_{N-1} - \mathbf{V}_N \rangle + \frac{\beta}{2} \|\mathbf{W}_N \mathbf{V}_{N-1} - \mathbf{V}_N\|^2, \end{aligned} \quad (7)$$

in which $\Psi_{2s} := (\{\text{vec}(\mathbf{W}_i)\}_{i=1}^N, \{\text{vec}(\mathbf{V}_i)\}_{i=1}^N, \text{vec}(\mathbf{\Lambda}))$, $\mathbf{\Lambda} \in \mathbb{R}^{d_N \times n}$ is the dual variable, parameter $\beta > 0$. Update subproblems of each block variable based on (7) in a Gauss-Seidel manner are listed in Table I, in which “P” (“PL”) represents the proximal (linearized) update, respectively. Based on Table I, the pseudocode of two-splitting RADMM training algorithms are given in Algorithm 1.

B. Convergence (Rate) of Two-Splitting RADMMs

In this section, we establish convergence and analyze the convergence rates of both the iteration points and objective function values for the serial and parallel two-splitting proximal RADMM algorithms presented in Algorithms 1 and 3.

Assumption 1 (Boundness). Parameters of the two-splitting proximal RADMM satisfy:

- $\beta > 1$,
- $\underline{\omega}_i \leq \omega_i^k \leq \bar{\omega}_i$ with some $0 < \underline{\omega}_i \leq \bar{\omega}_i, i \in [N-1]$,
- $\underline{\nu}_i \leq \nu_i^k \leq \bar{\nu}_i$ with some $0 < \underline{\nu}_i \leq \bar{\nu}_i, i \in [N-1]$.

Under Assumption 1, we have Proposition 1 and Proposition 2.

Proposition 1 (Proof in Appendix IX-D). $\mathcal{L}_\beta^{2s}(\Psi_{2s}^{k+1}) \leq \mathcal{L}_\beta^{2s}(\Psi_{2s}^k) - c_1 \|\Psi_{2s}^{k+1} - \Psi_{2s}^k\|^2$ with some $c_1 > 0$.

TABLE I
UPDATES OF BLOCK VARIABLES IN TWO-SPLITTING RADMMs.

| Variables | Updates |
|--------------------------|---------------------------------------------------------------------------------------------------------------------------------------------------------------------------------------------------------------------------------------------------------------------------------------------------------------------------------------------------------------------------------------------------------------------------------------------------------------------------------------------------------------------------------------------------------------------------------------------------------------------------------------------------------------------------------------------------------------------------------------------------------------------------------------------------------|
| \mathbf{W}_N^{k+1} | $(\beta \mathbf{V}_N^k - \mathbf{\Lambda}^k) \mathbf{V}_{N-1}^{k \top} (\lambda \mathbf{I} + \beta \mathbf{V}_{N-1}^k \mathbf{V}_{N-1}^{k \top})^{-1} \quad (8)$ |
| \mathbf{W}_i^{k+1} | $\text{P: } \arg \min_{\ \mathbf{W}_i\ \leq \varkappa} \left\{ \frac{\lambda}{2} \ \mathbf{W}_i\ ^2 + \frac{\omega_i^k}{2} \ \mathbf{W}_i - \mathbf{W}_i^k\ ^2 + \frac{\mu}{2} \ \mathbf{V}_{i-1}^k + \sigma_i(\mathbf{W}_i \mathbf{V}_{i-1}^k) - \mathbf{V}_i^k\ ^2 \right\} \quad (9)$ $\text{PL: } -\frac{\mu}{\lambda + \tau_i^k} [(\mathbf{V}_{i-1}^k + \sigma_i(\mathbf{W}_i \mathbf{V}_{i-1}^k) - \mathbf{V}_i^k) \odot \sigma'_i(\mathbf{W}_i \mathbf{V}_{i-1}^k)] \mathbf{V}_{i-1}^{k \top} + \frac{\tau_i^k}{\lambda + \tau_i^k} \mathbf{W}_i^k \quad (10)$ |
| \mathbf{V}_i^{k+1} | $\text{P: } \arg \min_{\mathbf{V}_i} \left\{ \frac{\mu}{2} \ \mathbf{V}_i + \sigma_{i+1}(\mathbf{W}_{i+1}^{k+1} \mathbf{V}_i) - \mathbf{V}_{i+1}^k\ _F^2 + \frac{\mu}{2} \ \mathbf{V}_{i-1}^{k+1} + \sigma_i(\mathbf{W}_i^{k+1} \mathbf{V}_{i-1}^{k+1}) - \mathbf{V}_i\ _F^2 + \frac{\nu_i^k}{2} \ \mathbf{V}_i - \mathbf{V}_i^k\ _F^2 \right\} \quad (11)$ $\text{PL: } \frac{\mu}{\mu + \nu_i^k} [\sigma_i(\mathbf{W}_i^{k+1} \mathbf{V}_{i-1}^{k+1}) + \mathbf{V}_{i-1}^{k+1} + \mathbf{V}_{i+1}^{k+1} - \mathbf{V}_i^k - \sigma_{i+1}(\mathbf{W}_{i+1}^{k+1} \mathbf{V}_i^k)] + \frac{\nu_i^k}{\mu + \nu_i^k} \mathbf{V}_i^k - \frac{\mu}{\mu + \nu_i^k} \mathbf{W}_{i+1}^{k+1 \top} [(\mathbf{V}_i^k - \mathbf{V}_{i+1}^k) \odot \sigma'_{i+1}(\mathbf{W}_{i+1}^{k+1} \mathbf{V}_i^k)] \quad (12)$ |
| \mathbf{V}_{N-1}^{k+1} | $\mu(\mu \mathbf{I} + \beta \mathbf{W}_N^{k+1 \top} \mathbf{W}_N^{k+1})^{-1} (\sigma_{N-1}(\mathbf{W}_{N-1}^{k+1} \mathbf{V}_{N-2}^{k+1}) + \mathbf{V}_{N-2}^{k+1}) + \beta(\mu \mathbf{I} + \beta \mathbf{W}_N^{k+1 \top} \mathbf{W}_N^{k+1})^{-1} \mathbf{W}_N^{k+1 \top} \mathbf{V}_N^k - (\mu \mathbf{I} + \beta \mathbf{W}_N^{k+1 \top} \mathbf{W}_N^{k+1})^{-1} \mathbf{W}_N^{k+1 \top} \mathbf{\Lambda}^k \quad (13)$ |
| \mathbf{V}_N^{k+1} | $\frac{1}{1 + \beta} (\mathbf{Y} + \beta \mathbf{W}_N^{k+1} \mathbf{V}_{N-1}^{k+1} + \mathbf{\Lambda}^k) \quad (14)$ |
| $\mathbf{\Lambda}^{k+1}$ | $\mathbf{\Lambda}^k + \beta(\mathbf{W}_N^{k+1} \mathbf{V}_{N-1}^{k+1} - \mathbf{V}_N^{k+1}) \quad (15)$ |

Proposition 2 (Proof in Appendix IX-E). $\|\nabla \mathcal{L}_\beta^{2s}(\Psi_{2s}^{k+1})\| \leq c_2 \|\Psi_{2s}^{k+1} - \Psi_{2s}^k\|$ with some $c_2 > 0$.

Our two main convergence results on the two-splitting proximal RADMM are shown in Theorem 1 and Theorem 2.

Theorem 1 (Convergence, proof in Appendix IX-F). $\Psi_{2s}^* \rightarrow \Psi_{2s}^*$ and $\mathcal{L}_\beta^{2s}(\Psi_{2s}^k) \rightarrow \mathcal{L}_\beta^{2s}(\Psi_{2s}^*)$. Ψ_{2s}^* is a KKT point of (6).

Theorem 1 guarantees the convergence of both iteration point and objective function value sequences. Specifically, the limit of the iteration is a KKT point.

Theorem 2 (Convergence Rate, proof in Appendix IX-F). Let θ be the KL exponent of \mathcal{L}_β^{2s} at Ψ_{2s}^* .

1. (R-linear) If $\theta = \frac{1}{2}$, then there exist $k_0 \in \mathbb{N}$, $\eta \in (0, 1)$ and

Algorithm 1: Two-Splitting RADMMs

Input: $\mathbf{X}, \mathbf{Y}, K, \lambda, \mu, \beta, \{\omega_i^k\}_{i=1}^{N-1}, \{\nu_i^k\}_{i=1}^{N-1}$, and $\{\mathbf{W}_i^0\}_{i=1}^N$.
 $\mathbf{V}_0^k \leftarrow \mathbf{X}, \mathbf{V}_i^0 \leftarrow \mathbf{V}_{i-1}^0 + \sigma_i(\mathbf{W}_i^0 \mathbf{V}_{i-1}^0), i \in [N-1]$,
 $\mathbf{V}_N^0 \leftarrow \mathbf{W}_N^0 \mathbf{V}_{N-1}^0, \mathbf{\Lambda}^0 \leftarrow \mathbf{0}$.
for $k \leftarrow 0$ to $K-1$ **do**
 Update \mathbf{W}_N^{k+1} by iteration equation (8).
 for $i \leftarrow N-1$ to **do**
 Update \mathbf{W}_i^{k+1} by solving (9) in proximal RADMM (by iteration equation (10) in proximal linearized RADMM).
 end
 for $i \leftarrow 1$ to $N-2$ **do**
 Update \mathbf{V}_i^{k+1} by solving (11) in proximal RADMM (by iteration equation (12) in proximal linearized RADMM).
 end
 Update \mathbf{V}_{N-1}^{k+1} by iteration equation (13).
 Update \mathbf{V}_N^{k+1} by iteration equation (14).
 Update $\mathbf{\Lambda}^{k+1}$ by iteration equation (15).
end
Output: $\{\mathbf{W}_i^K\}_{i=1}^N$.

$c > 0$ such that for each $k \geq k_0$, we have

- $\|\Psi_{2s}^k - \Psi_{2s}^*\| \leq c\eta^{k-k_0+1}$,
- $\mathcal{L}_\beta^{2s}(\Psi_{2s}^k) - \mathcal{L}_\beta^{2s}(\Psi_{2s}^*) \leq c\eta^{k-k_0+1}$.

2. (R-sublinear) If $\theta \in (\frac{1}{2}, 1)$, then there exist $k_0 \in \mathbb{N}$ and $c > 0$ such that for each $k \geq k_0$,

- $\|\Psi_{2s}^k - \Psi_{2s}^*\| \leq c(k - k_0 + 1)^{\frac{1-\theta}{1-2\theta}}$,
- $\mathcal{L}_\beta^{2s}(\Psi_{2s}^k) - \mathcal{L}_\beta^{2s}(\Psi_{2s}^*) \leq c(k - k_0 + 1)^{-\frac{1}{2\theta-1}}$.

Theorem 2 implies the *R-linear* and $\mathcal{O}(k^{\frac{1-\theta}{1-2\theta}})$ ($\mathcal{O}(k^{-\frac{1}{2\theta-1}})$) *R-sublinear* convergence rate of the iteration point (objective function value) sequences generated by the proximal two-splitting RADMM training algorithms.

V. THREE-SPLITTING RADMMs

In this section, to facilitate the efficient training of deeper residual networks, we design and discuss scalable three-splitting proximal (linearized) RADMM training algorithms.

A. Three-Splitting Proximal (Linearized) RADMMs

Clearly, the three-splitting approximation (4) with MSE loss, ridge regression penalty, and identity mapping $h_i, i \in [N-1]$ is as below.

$$\begin{aligned} & \min_{\mathbf{W}, \mathbf{U}, \mathbf{V}} \mathcal{J}(\mathbf{W}, \mathbf{V}_N) + \frac{\mu}{2} \sum_{i=1}^{N-1} \|\mathbf{V}_{i-1} + \sigma_i(\mathbf{U}_i) - \mathbf{V}_i\|^2 \\ & \text{s.t. } \mathbf{U}_i = \mathbf{W}_i \mathbf{V}_{i-1}, i \in [N-1], \\ & \mathbf{V}_N = \mathbf{W}_N \mathbf{V}_{N-1}, \end{aligned} \quad (16)$$

where $\mathbf{U}_i = (\mathbf{u}_i^1, \dots, \mathbf{u}_i^n)$ for $i \in [N-1]$, $\mathbf{U} := (\text{vec}(\mathbf{U}_1), \dots, \text{vec}(\mathbf{U}_{N-1}))$, whose augmented Lagrangian function is

$$\begin{aligned} \mathcal{L}_\beta^{3s}(\Psi_{3s}) &:= \mathcal{J}(\mathbf{W}, \mathbf{V}_N) + \frac{\mu}{2} \sum_{i=1}^{N-1} \|\mathbf{V}_{i-1} + \sigma_i(\mathbf{U}_i) - \mathbf{V}_i\|^2 \\ &+ \sum_{i=1}^{N-1} (\langle \mathbf{\Lambda}_i, \mathbf{W}_i \mathbf{V}_{i-1} - \mathbf{U}_i \rangle + \frac{\beta_i}{2} \|\mathbf{W}_i \mathbf{V}_{i-1} - \mathbf{U}_i\|^2) \\ &+ \langle \mathbf{\Lambda}_N, \mathbf{W}_N \mathbf{V}_{N-1} - \mathbf{V}_N \rangle + \frac{\beta_N}{2} \|\mathbf{W}_N \mathbf{V}_{N-1} - \mathbf{V}_N\|^2, \end{aligned} \quad (17)$$

in which $\Psi_{3s} := (\{\text{vec}(\mathbf{W}_i)\}_{i=1}^N, \{\text{vec}(\mathbf{V}_i)\}_{i=1}^N, \{\text{vec}(\mathbf{\Lambda}_i)\}_{i=1}^N, \{\text{vec}(\mathbf{U}_i)\}_{i=1}^{N-1})$, $\{\mathbf{\Lambda}_i\}_{i=1}^{N-1} \subseteq \mathbb{R}^{d \times n}$ and $\mathbf{\Lambda}_N \in \mathbb{R}^{q \times n}$ are dual variables, parameters $\beta_i > 0, i \in [N]$. Update subproblems of each block variable based on (17) in a Gauss-Seidel

manner are listed in Table II. After that, the pseudocode of three-splitting proximal (linearized) RADMM training algorithms are given in Algorithm 2.

TABLE II
UPDATES OF BLOCK VARIABLES IN THREE-SPLITTING RADMMs.

| Variables | Updates |
|----------------------------|------------------------------------------------------------------------------------------------------------------------------------------------------------------------------------------------------------------------------------------------------------------------------------------------------------------------------------------------------------------------------------------------------------------------------------------------------------------------------------------------------------------------------------------------------------------------|
| \mathbf{W}_N^{k+1} | $(\beta_N \mathbf{V}_N^k - \mathbf{\Lambda}_N^k) \mathbf{V}_{N-1}^{k \top} (\lambda \mathbf{I} + \beta_N \mathbf{V}_{N-1}^k \mathbf{V}_{N-1}^{k \top})^{-1} \quad (18)$ |
| \mathbf{W}_i^{k+1} | $(\beta_i \mathbf{U}_i^k - \mathbf{\Lambda}_i^k) \mathbf{V}_{i-1}^{k \top} (\lambda \mathbf{I} + \beta_i \mathbf{V}_{i-1}^k \mathbf{V}_{i-1}^{k \top})^{-1} \quad (19)$ |
| \mathbf{U}_i^{k+1} | $\begin{aligned} \mathbf{P}: & \arg \min_{\mathbf{U}_i} \left\{ \frac{\mu}{2} \ \mathbf{V}_{i-1}^{k+1} + \sigma_i(\mathbf{U}_i) - \mathbf{V}_i^k\ ^2 \right. \\ &+ \frac{\beta_i}{2} \ \mathbf{U}_i - \mathbf{W}_i^{k+1} \mathbf{V}_{i-1}^{k+1} - \frac{1}{\beta_i} \mathbf{\Lambda}_i^k\ ^2 \\ &+ \left. \frac{\omega_i^k}{2} \ \mathbf{U}_i - \mathbf{U}_i^k\ ^2 \right\} \end{aligned} \quad (20)$ |
| \mathbf{V}_i^{k+1} | $\begin{aligned} \mathbf{PL}: & -\frac{\mu}{\tau_i^k + \beta_i} (\mathbf{V}_{i-1}^{k+1} + \sigma_i(\mathbf{U}_i^k) - \mathbf{V}_i^k) \odot \\ & \sigma'_i(\mathbf{U}_i^k) + \frac{\tau_i^k}{\tau_i^k + \beta_i} \mathbf{U}_i^k + \frac{1}{\tau_i^k + \beta_i} \mathbf{\Lambda}_i^k \\ &+ \frac{\beta_i}{\tau_i^k + \beta_i} \mathbf{W}_i^{k+1} \mathbf{V}_{i-1}^{k+1} \end{aligned} \quad (21)$ |
| \mathbf{V}_{N-1}^{k+1} | $\begin{aligned} & \mu(2\mu\mathbf{I} + \beta_{i+1} \mathbf{W}_{i+1}^{k+1 \top} \mathbf{W}_{i+1}^{k+1})^{-1} (\mathbf{V}_{i-1}^{k+1} + \mathbf{V}_{i+1}^k) \\ & - \sigma_{i+1}(\mathbf{U}_{i+1}^k) + \sigma_i(\mathbf{U}_i^{k+1}) + \beta_{i+1}(2\mu\mathbf{I} + \\ & \beta_{i+1} \mathbf{W}_{i+1}^{k+1 \top} \mathbf{W}_{i+1}^{k+1})^{-1} \mathbf{W}_{i+1}^{k+1 \top} \mathbf{U}_{i+1}^k \\ & - (2\mu\mathbf{I} + \beta_{i+1} \mathbf{W}_{i+1}^{k+1 \top} \mathbf{W}_{i+1}^{k+1})^{-1} \mathbf{W}_{i+1}^{k+1 \top} \mathbf{\Lambda}_{i+1}^k \end{aligned} \quad (22)$ |
| \mathbf{V}_{N-1}^{k+1} | $\begin{aligned} & \mu(\mu\mathbf{I} + \beta_N \mathbf{W}_N^{k+1 \top} \mathbf{W}_N^{k+1})^{-1} (\sigma_{N-1}(\mathbf{U}_{N-1}^{k+1}) \\ & + \mathbf{V}_{N-2}^{k+1}) + \beta_N(\mu\mathbf{I} + \beta_N \mathbf{W}_N^{k+1 \top} \mathbf{W}_N^{k+1})^{-1} \\ & \mathbf{W}_N^{k+1 \top} \mathbf{V}_N^k - (\mu\mathbf{I} + \beta_N \mathbf{W}_N^{k+1 \top} \mathbf{W}_N^{k+1})^{-1} \\ & \mathbf{W}_N^{k+1 \top} \mathbf{\Lambda}_N^k \end{aligned} \quad (23)$ |
| \mathbf{V}_N^{k+1} | $\frac{1}{1 + \beta_N} (\mathbf{Y} + \beta_N \mathbf{W}_N^{k+1} \mathbf{V}_{N-1}^{k+1} + \mathbf{\Lambda}_N^k) \quad (24)$ |
| $\mathbf{\Lambda}_i^{k+1}$ | $\mathbf{\Lambda}_i^k + \beta_i (\mathbf{W}_i^{k+1} \mathbf{V}_{i-1}^{k+1} - \mathbf{U}_i^{k+1}) \quad (25)$ |
| $\mathbf{\Lambda}_N^{k+1}$ | $\mathbf{\Lambda}_N^k + \beta_N (\mathbf{W}_N^{k+1} \mathbf{V}_{N-1}^{k+1} - \mathbf{V}_N^{k+1}) \quad (26)$ |

B. Convergence (Rate) of Three-Splitting RADMMs

In this section, we establish convergence and derive convergence rate estimates for both the iteration points and the objective function values of the serial and parallel three-splitting proximal RADMMs. The challenges encountered in the theoretical analysis and our proof outline are discussed in Section V-B1 and Section V-B2, respectively, with the principal results presented in Section V-B3.

Algorithm 2: Three-Splitting RADMMs

Input: $\mathbf{X}, \mathbf{Y}, K, \lambda, \mu, \{\beta_i\}_{i=1}^N, \{\omega_i^k\}_{i=1}^{N-1}$, and $\{\mathbf{W}_i^0\}_{i=1}^N$.
 $\mathbf{V}_0^k \leftarrow \mathbf{X}$, $\mathbf{U}_i^0 \leftarrow \mathbf{W}_i^0 \mathbf{V}_{i-1}^0$, $\mathbf{V}_i^0 \leftarrow \mathbf{V}_{i-1}^0 + \sigma_i(\mathbf{U}_i^0)$,
 $i \in [N-1]$, $\mathbf{V}_N^0 \leftarrow \mathbf{W}_N^0 \mathbf{V}_{N-1}^0$, and $\mathbf{\Lambda}_i^0 \leftarrow \mathbf{0}$, $i \in [N]$.
for $k \leftarrow 0$ **to** $K-1$ **do**
 Update \mathbf{W}_N^{k+1} by iteration equation (18).
 for $i \leftarrow N-1$ **to** 1 **do**
 | Update \mathbf{W}_i^{k+1} by iteration equation (19).
 end
 for $i \leftarrow 1$ **to** $N-2$ **do**
 | Update \mathbf{U}_i^{k+1} by solving (20) in proximal RADMM (by iteration equation (21) in proximal linearized RADMM).
 | Update \mathbf{V}_i^{k+1} by iteration equation (22).
 end
 Update \mathbf{U}_{N-1}^{k+1} by solving (20) in proximal RADMM (by iteration equation (21) in proximal linearized RADMM).
 Update \mathbf{V}_{N-1}^{k+1} by iteration equation (23).
 Update \mathbf{V}_N^{k+1} by iteration equation (24).
 for $i \leftarrow 1$ **to** $N-1$ **do**
 | Update $\mathbf{\Lambda}_i^{k+1}$ by iteration equation (25).
 end
 Update $\mathbf{\Lambda}_N^{k+1}$ by iteration equation (26).
end
Output: $\{\mathbf{W}_i^K\}_{i=1}^N$.

1) *Regularized Augmented Lagrangian:* Unfortunately, different from the \mathcal{L}_β^{2s} , it is difficult to realize a sufficient descent for \mathcal{L}_β^{3s} directly. To deal with this issue, we first construct a regularization \mathcal{L}_R^{3s} for the augmented Lagrangian function:

$$\mathcal{L}_R^{3s}(\tilde{\Psi}_{3s}) := \mathcal{L}_\beta^{3s}(\Psi_{3s}) + \sum_{i=1}^{N-1} \theta_i \|\mathbf{U}_i - \tilde{\mathbf{U}}_i\|^2 + \sum_{i=1}^{N-1} \eta_i \|\mathbf{V}_i - \tilde{\mathbf{V}}_i\|^2,$$

where $\tilde{\Psi}_{3s} := (\Psi_{3s}, \{\text{vec}(\tilde{\mathbf{U}}_i)\}_{i=1}^{N-1}, \{\text{vec}(\tilde{\mathbf{V}}_i)\}_{i=1}^{N-1})$, $\theta_i := \frac{4(\omega_i)^2}{\beta_i} + \frac{\omega_i}{4}$, $\eta_i := \frac{4\mu^2\psi_i^2}{\beta_i} + \frac{\mu}{4}$, $i \in [N-1]$. We define the iteration $\tilde{\mathbf{U}}_i^k := \mathbf{U}_i^{k-1}$, $\tilde{\mathbf{V}}_i^k := \mathbf{V}_i^{k-1}$, $i \in [N-1]$. Similarly with the discussion on two-splitting RADMMs in Section IV-B, we can prove that (see Lemma 1)

$$\tilde{\Psi}_{3s}^k \rightarrow \tilde{\Psi}_{3s}^*, \mathcal{L}_R^{3s}(\tilde{\Psi}_{3s}^k) \rightarrow \mathcal{L}_R^{3s}(\tilde{\Psi}_{3s}^*), \nabla \mathcal{L}_R^{3s}(\tilde{\Psi}_{3s}^*) = \mathbf{0};$$

$$\|\tilde{\Psi}_{3s}^k - \tilde{\Psi}_{3s}^*\| = \mathcal{O}(\eta^k) (\mathcal{O}(k^{\frac{1-\theta}{1-2\theta}})),$$

$$\mathcal{L}_R^{3s}(\tilde{\Psi}_{3s}^k) - \mathcal{L}_R^{3s}(\tilde{\Psi}_{3s}^*) = \mathcal{O}(\eta^k) (\mathcal{O}(k^{-\frac{1}{2\theta-1}})).$$

2) *Connections between $\mathcal{L}_\beta^{3s}(\Psi_{3s})$ and $\mathcal{L}_R^{3s}(\tilde{\Psi}_{3s})$:* We can prove that

$$\begin{aligned} \|\Psi_{3s}^k - \Psi_{3s}^*\| &\leq \|\tilde{\Psi}_{3s}^k - \tilde{\Psi}_{3s}^*\|, \\ \mathcal{L}_\beta^{3s}(\Psi_{3s}^k) - \mathcal{L}_\beta^{3s}(\Psi_{3s}^*) &\leq \mathcal{L}_R^{3s}(\tilde{\Psi}_{3s}^k) - \mathcal{L}_R^{3s}(\tilde{\Psi}_{3s}^*). \end{aligned} \quad (27)$$

Then the convergence of $\{\tilde{\Psi}_{3s}^k\}$ and $\{\mathcal{L}_R^{3s}(\tilde{\Psi}_{3s}^k)\}$ imply that of $\{\Psi_{3s}^k\}$ and $\{\mathcal{L}_\beta^{3s}(\Psi_{3s}^k)\}$. In addition, we have $\nabla \mathcal{L}_R^{3s}(\tilde{\Psi}_{3s}^*) = \mathbf{0}$, and for each $i \in [N-1]$,

$$\frac{\partial \mathcal{L}_R^{3s}}{\partial \mathbf{U}_i}(\tilde{\Psi}_{3s}^*) = \frac{\partial \mathcal{L}_\beta^{3s}}{\partial \mathbf{U}_i}(\Psi_{3s}^*), \quad \frac{\partial \mathcal{L}_R^{3s}}{\partial \mathbf{V}_i}(\tilde{\Psi}_{3s}^*) = \frac{\partial \mathcal{L}_\beta^{3s}}{\partial \mathbf{V}_i}(\Psi_{3s}^*). \quad (28)$$

Thus it can be proved that the limit Ψ_{3s}^* is a KKT point (see Theorem 3). Furthermore, the same convergence rate can also be guaranteed (see Theorem 4). Relationship between $\mathcal{L}_\beta^{3s}(\Psi_{3s})$ and $\mathcal{L}_R^{3s}(\tilde{\Psi}_{3s})$ is shown in Figure 2.

3) *Convergence results:* Boundness assumption is first given in Assumption 2.

Assumption 2 (Boundness). *Parameters of the three-splitting proximal RADMM satisfy:*

- $\beta_i > \underline{\beta}_i$ with some $\underline{\beta}_i, i \in [N]$,

Eq. (27), Convergence (Rate)



Fig. 2. Relationship between $\mathcal{L}_\beta^{3s}(\Psi_{3s})$ and $\mathcal{L}_R^{3s}(\tilde{\Psi}_{3s})$.

- $\underline{\omega}_i < \omega_i^k \leq \omega_i^{k+1} < \bar{\omega}_i$ with some $\underline{\omega}_i < \bar{\omega}_i, i \in [N-1]$.

See Appendix IX-A for the values of $\{\underline{\beta}_i\}_{i=1}^N$, $\{\omega_i\}_{i=1}^{N-1}$, and $\{\bar{\omega}_i\}_{i=1}^{N-1}$. Moreover, we assume the upper boundedness $\|\mathbf{V}_i^k\| \leq \bar{\mathcal{V}}_i$ with some $\bar{\mathcal{V}}_i > 0, i \in [N-1]$. Under these assumptions, we first have Lemma 1 about \mathcal{L}_R^{3s} and $\tilde{\Psi}_{3s}$.

Lemma 1 (Proof in Appendix IX-H).

$$\tilde{\Psi}_{3s}^k \rightarrow \tilde{\Psi}_{3s}^*, \mathcal{L}_R^{3s}(\tilde{\Psi}_{3s}^k) \rightarrow \mathcal{L}_R^{3s}(\tilde{\Psi}_{3s}^*).$$

1. If the KL exponent θ of \mathcal{L}_R^{3s} at $\tilde{\Psi}_{3s}^*$ is equal to $\frac{1}{2}$, then there exist $k_0 \in \mathbb{N}$, $\eta \in (0, 1)$ and $c > 0$ such that for each $k \geq k_0$, we have $\|\tilde{\Psi}_{3s}^k - \tilde{\Psi}_{3s}^*\| \leq c\eta^{k-k_0+1}$, and $\mathcal{L}_R^{3s}(\tilde{\Psi}_{3s}^k) - \mathcal{L}_R^{3s}(\tilde{\Psi}_{3s}^*) \leq c\eta^{k-k_0+1}$.
2. If $\theta \in (\frac{1}{2}, 1)$, then there exist $k_0 \in \mathbb{N}$ and $c > 0$ such that for each $k \geq k_0$, we have $\|\tilde{\Psi}_{3s}^k - \tilde{\Psi}_{3s}^*\| \leq c(k - k_0 + 1)^{\frac{1-\theta}{1-2\theta}}$, and $\mathcal{L}_R^{3s}(\tilde{\Psi}_{3s}^k) - \mathcal{L}_R^{3s}(\tilde{\Psi}_{3s}^*) \leq c(k - k_0 + 1)^{-\frac{1}{2\theta-1}}$.

Our main convergence results of the three-splitting proximal RADMMs are shown in Theorem 3 and Theorem 4.

Theorem 3 (Convergence, proof in Appendix IX-H). $\Psi_{3s}^k \rightarrow \Psi_{3s}^*$ and $\mathcal{L}_\beta^{3s}(\Psi_{3s}^k) \rightarrow \mathcal{L}_\beta^{3s}(\Psi_{3s}^*)$. Ψ_{3s}^* is a KKT point of (16).

Theorem 4 (Convergence rate, proof in Appendix IX-H). *Convergence rate of the three-splitting proximal RADMM:*

1. (R-linear) If the KL exponent $\theta = \frac{1}{2}$, then there exist $k_0 \in \mathbb{N}$, $\eta \in (0, 1)$ and $c > 0$ such that for each $k \geq k_0$, we have
 - $\|\Psi_{3s}^k - \Psi_{3s}^*\| \leq c\eta^{k-k_0+1}$,
 - $\mathcal{L}_\beta^{3s}(\Psi_{3s}^k) - \mathcal{L}_\beta^{3s}(\Psi_{3s}^*) \leq c\eta^{k-k_0+1}$.
2. (R-sublinear) If $\theta \in (\frac{1}{2}, 1)$, then there exist $k_0 \in \mathbb{N}$ and $c > 0$ such that for each $k \geq k_0$,
 - $\|\Psi_{3s}^k - \Psi_{3s}^*\| \leq c(k - k_0 + 1)^{\frac{1-\theta}{1-2\theta}}$,
 - $\mathcal{L}_\beta^{3s}(\Psi_{3s}^k) - \mathcal{L}_\beta^{3s}(\Psi_{3s}^*) \leq c(k - k_0 + 1)^{-\frac{1}{2\theta-1}}$.

VI. PARALLEL AND DISTRIBUTED ALGORITHMS

In this section, we develop the parallel/distributed RADMM training algorithms and theoretically demonstrate their advantages in terms of reduced time complexity and lower per-node runtime memory requirements.

A. Parallel RADMMs

Note that for each residual block in the network, updating its block variables requires only the block variables from its immediately adjacent block(s), which presents an opportunity for model parallelism. We refer to this scheme as the parallel regional update (PRU), where “regional” highlights this localized update characteristic. As illustrated in Figure 3, the arrows indicate the communication between adjacent processors (or blocks). In contrast, BP-based methods necessitate that the

gradient be sequentially propagated through all blocks, thereby limiting scalability. With PRU, we can assign N parallel processors, each responsible for updating the block variables of a single residual block. Based on this observation, we

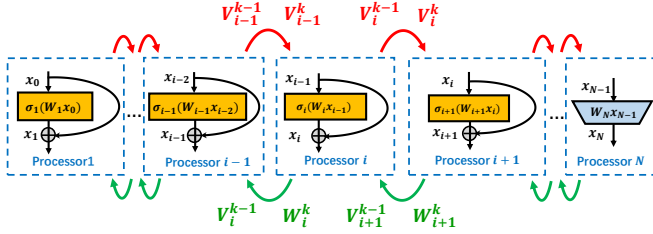


Fig. 3. PRU employed in parallel RADMMs.

propose parallel RADMM training algorithms derived from our serial version. In our approach, a processor initiates the update of its assigned block as soon as the necessary block variables from the adjacent block(s) become available. Note that the N processors operate asynchronously, as a processor must wait to retrieve a variable from another until it has been updated. However, such waiting does not fully serialize the updates, rather, it produces a pipelined update pattern that improves the time complexity relative to the serial version (see Section VI-B). The implementation strategy and details are provided in Section VII-B.

Algorithm 3: Parallel Two-Splitting RADMMs

```

Input:  $\mathbf{X}, \mathbf{Y}, K, \lambda, \mu, \beta, \{\omega_i^k\}_{i=1}^{N-1}, \{V_i^k\}_{i=1}^{N-1}$ , and  $\{\mathbf{W}_i^0\}_{i=1}^N$ .
 $\mathbf{V}_0^k \leftarrow \mathbf{X}, \mathbf{V}_0^0 \leftarrow \mathbf{V}_{i-1}^0 + \sigma_i(\mathbf{W}_i^0 \mathbf{V}_{i-1}^0), i \in [N-1]$ ,
 $\mathbf{V}_N^0 \leftarrow \mathbf{W}_N^0 \mathbf{V}_{N-1}^0$  and  $\mathbf{\Lambda}^0 \leftarrow \mathbf{0}$ .
parallel_for  $i \in [N]$  do
  for  $k \leftarrow 0$  to  $K-1$  do
    if  $i < N$  then
      Update  $\mathbf{W}_i^{k+1}$  by solving (9) in proximal RADMM
      (by iteration equation (10) in proximal linearized
      RADMM).
    else
      Update  $\mathbf{W}_N^{k+1}$  by iteration equation (8).
    end
    if  $i < N$  then Retrieve necessary block variables from
    processor  $i+1$ ;
    if  $i > 1$  then Retrieve necessary block variables from
    processor  $i-1$ ;
    if  $i < N-1$  then
      Update  $\mathbf{V}_i^{k+1}$  by solving (11) in proximal RADMM
      (by iteration equation (12) in proximal linearized
      RADMM).
    else if  $i = N-1$  then
      Update  $\mathbf{V}_{N-1}^{k+1}$  by iteration equation (23).
    else
      Update  $\mathbf{V}_N^{k+1}$  by iteration equation (24).
    end
    if  $i = N$  then
      Update  $\mathbf{\Lambda}^{k+1}$  by iteration equation (15).
    end
  end
  Synchronize all processors.
Output:  $\{\mathbf{W}_i^K\}_{i=1}^N$ .

```

B. Lower Time Complexity

To demonstrate the reduced time complexity of our parallel version, we compare the time complexities of the serial and

parallel proximal linearized RADMMs. For illustration, Figure 7 depicts a pipelined update pattern for the parallel RADMMs. In this figure, the horizontal axis represents runtime, where each unit of time corresponds to the update duration for a single block variable. Each row represents the update sequence for one block variable, and in the leftmost column, block variables grouped within the same box are updated by the same processor. The number in each block indicates the epoch during which the corresponding variable is updated.

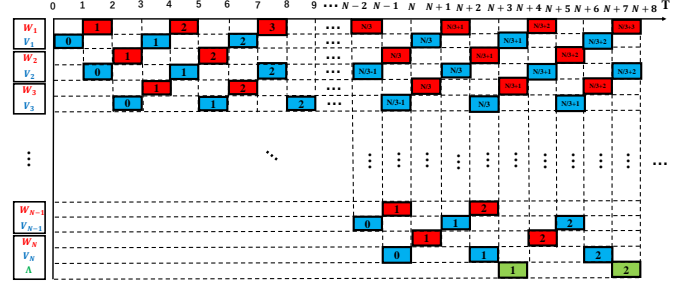


Fig. 4. Pipelined update pattern of the parallel two-splitting RADMMs.

Let $T_{\text{mul}}(n)$ denote the computational complexity of multiplying two $n \times n$ matrices, and let $T_{\text{comm}}(K, N, d, q, n)$ denote the communication cost incurred by processors during K updates. Here, basic operations include addition, subtraction, multiplication, division, and the evaluation of activation functions. Let $\tau = \max\{d, q, n\}$. According to recent studies on the time complexity of matrix multiplication [43], the cost of square matrix multiplication constitutes the primary bottleneck in updating block variables. Therefore, the time complexity for each block variable update is $\mathcal{O}(T_{\text{mul}}(\tau))$.

1) *Serial RADMMs*: The time complexities of serial proximal RADMM training algorithms are both $\mathcal{O}(KNT_{\text{mul}}(\tau))$.

2) *Parallel RADMMs*: Based on the pipeline shown in Figure 7, the time complexities of the parallel RADMMs are

$$\mathcal{O}(\max\{K, N\}T_{\text{mul}}(\tau)) + \mathcal{O}(T_{\text{comm}}(K, N, d, q, n)).$$

If the communication cost is relatively small, i.e.,

$$\max\{K, N\}T_{\text{mul}}(\tau) = \mathcal{O}(T_{\text{comm}}(K, N, d, q, n)),$$

our parallelization via PRU can reduce the time complexity from $\mathcal{O}(KNT_{\text{mul}}(\tau))$ to $\mathcal{O}(\max\{K, N\}T_{\text{mul}}(\tau))$.

C. Less Runtime Memory Requirement

In this section, we theoretically demonstrate the scalability of our distribution strategy. As noted in Section I, BP-based methods do not exhibit this property. Under our approach, each node stores only the block variables corresponding to its assigned residual block, thereby substantially reducing the per-node memory footprint. Consequently, the distributed implementation of our parallel algorithms significantly alleviates memory constraints.

1) *Serial RADMMs*: For the serial algorithms, all variables are stored on a single processor, and only the iteration values from two consecutive steps need to be retained. Consequently, the runtime memory requirement for the serial RADMMs is $\mathcal{O}(N \max\{d, q\} \max\{d, n\})$.

2) *Distributed RADMMs*: In the distributed configuration, only the block variables allocated to each node are stored in its runtime memory. The per-node runtime memory requirements of the parallel RADMMs are summarized below, where processor i corresponds to the i th layer of the residual network:

- Processors $1, \dots, N-2$: $\mathcal{O}(d \max\{d, n\})$,
- Processor $N-1$: $\mathcal{O}(\max\{d, q\} \max\{d, n\})$,
- Processor N : $\mathcal{O}(\max\{q \max\{d, n\}, dn\})$.

Therefore, we know that the distributed algorithm can reduce the per-node runtime memory requirement from *cubic* to *quadratic* complexity.

VII. EXPERIMENTS

We compare our proximal linearized RADMMs with several well-known BP-based algorithms (SGD, SGDM, Adam) on the Wine Quality dataset² to demonstrate the fast and stable convergence, superior performance, and enhanced speed offered by our algorithms in Section VII-A. Furthermore, the advantages of our parallel RADMMs are presented in Section VII-B. Detailed experimental settings are provided in Appendix IX-C.

A. Wine Quality Dataset

In this section, we present experimental results on the Wine Quality dataset, demonstrating the fast and stable convergence, superior performance, and enhanced computational speed of our proximal linearized RADMM training algorithms.

1) *Fast and Stable Convergence*: We employ a 40-layer residual network to demonstrate the fast and stable convergence of our RADMM algorithms. Figure 5 presents the MSE for both training and testing losses for each algorithm after 600 iterations³. The results clearly indicate that our RADMMs converge rapidly with minimal fluctuations for networks utilizing both ReLU and sigmoid activations. Specifically, for the ReLU activation network, our RADMMs substantially outperform SGD, SGDM, and Adam by achieving lower MSE values and faster convergence. Similarly, for the sigmoid activation network, both the two- and three-splitting RADMM training algorithms attain lower MSE losses compared to SGD and SGDM, and perform comparably to Adam.

2) *Superior Performance*: In this section, we compare the performance of our RADMM algorithms with SGD, SGDM, and Adam for training both relatively shallow and deep networks using ReLU or sigmoid activations, respectively. After 600 iterations, Table III presents the MSE test loss for residual networks of various depths. The two smallest losses are highlighted in bold, and a hyphen (“-”) denotes an MSE test loss exceeding 500. For the ReLU network training task, our RADMMs significantly outperform the BP-based algorithms on deep networks (i.e., 20-, 30-, and 40-layer residual networks), with our three-splitting RADMM achieving the lowest MSE test loss on the 30- and 40-layer networks. For networks employing sigmoid activation, the three-splitting RADMM outperforms the two-splitting RADMM,

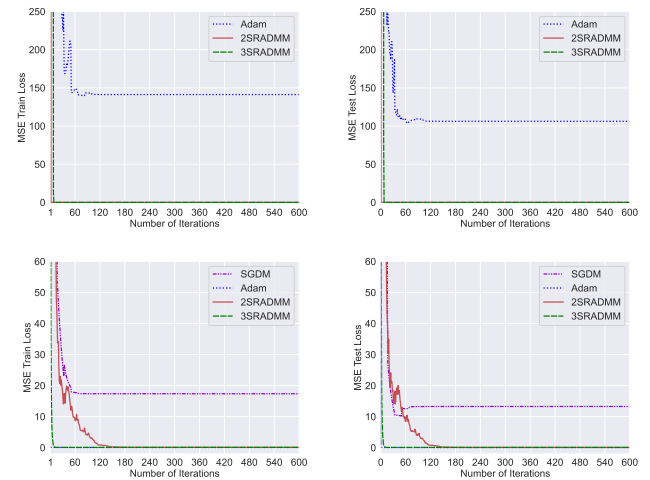


Fig. 5. MSE train (left), test (right) losses for the 40-layer ReLU (up), sigmoid (down) residual network on Wine Quality dataset.

and its performance is only marginally inferior to the best result obtained by Adam. In summary, benefiting from the ability to circumvent the exploding gradient issue, both the two- and three-splitting RADMM algorithms perform well on deep networks, with the three-splitting variant generally yielding lower MSE test losses than the two-splitting variant in most scenarios.

TABLE III
MEAN SQUARED ERROR TEST LOSSES

| Loss \ Algo | SGD | SGDM | Adam | 2SRADMM | 3SRADMM |
|----------------|----------|---------------|---------------|---------------|---------------|
| ReLU | | | | | |
| 3 | 0.2951 | 0.2951 | 0.0656 | 0.0668 | 0.0941 |
| 10 | 301.7660 | 301.7660 | 0.0652 | 0.0657 | 0.0640 |
| 20 | - | - | 0.1357 | 0.0705 | 0.0729 |
| 30 | - | - | 1.4892 | 0.0864 | 0.0708 |
| 40 | - | - | 106.2628 | 0.0844 | 0.0725 |
| Sigmoid | | | | | |
| 3 | 0.0629 | 0.0586 | 0.0579 | 0.0593 | 0.0579 |
| 10 | 0.0598 | 0.0596 | 0.0569 | 0.0606 | 0.0626 |
| 20 | 2.2278 | 6.1277 | 0.0556 | 0.0848 | 0.0595 |
| 30 | - | 0.0697 | 0.0574 | 0.1114 | 0.0647 |
| 40 | - | 13.2671 | 0.0577 | 0.0725 | 0.0688 |

3) *Enhanced Speed*: After 5 runs each with 600 iterations, the means and standard deviations of runtime of RADMMs, SGD, SGDM and Adam for 3-layer ReLU and sigmoid residual networks training on Wine Quality dataset are shown in Figure 6, in which the standard deviation is reflected by the length of each error bar above and below the mean value. Our two-splitting RADMM has the highest speed in the 5 algorithms on both ReLU and sigmoid networks. Besides, the runtimes of three-splitting RADMM on ReLU and sigmoid networks are acceptable and lower than those of Adam.

B. Parallel Implementation

To better illustrate the time complexity benefits of parallelization, we design and implement a control protocol for the parallel proximal linearized RADMM algorithm (see Algorithm 3) using Python’s multiprocessing and interprocess communication (IPC). In our implementation, the main procedure and the coordinator reside in a single process, while

²<https://archive.ics.uci.edu/dataset/186/wine+quality>

³The number of iterations in the experiments in this paper is equal to the number of updates divided by the number of batches in the train set.

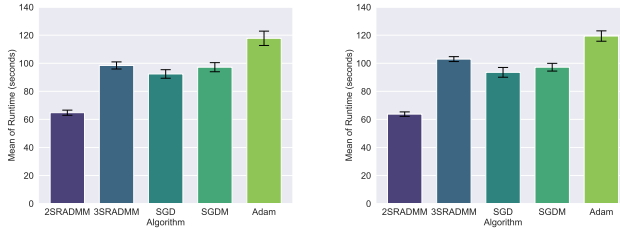


Fig. 6. Runtime for the 3-layer ReLU (left), sigmoid (right) residual network on Wine Quality dataset.

each network layer is assigned to its own subprocess. Communication among these processes is facilitated by message queues to transfer data and control signals. Figure 7 presents a UML sequence diagram for a 3-layer network ($N = 3$) as an example of this setup. Notably, our protocol can be easily extended to larger-scale tasks, such as multi-node clusters, by replacing the IPC mechanism with alternatives such as RPC.

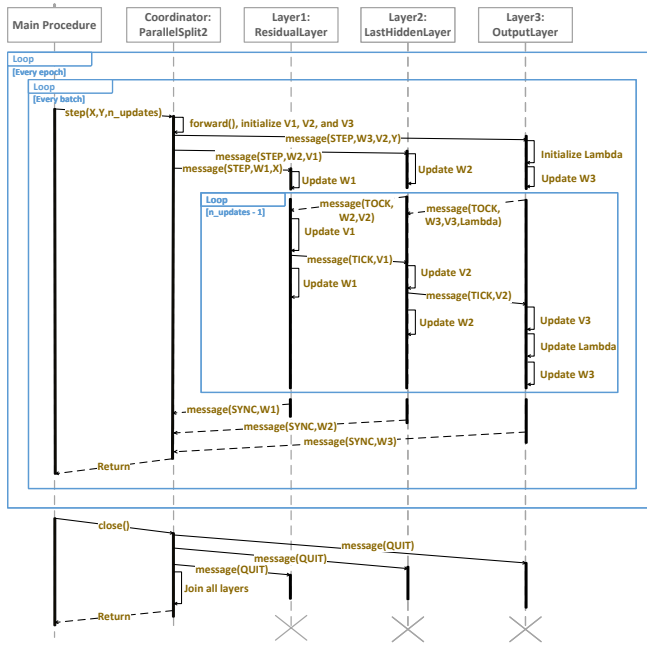


Fig. 7. UML sequence diagram for PRU parallel training, taking a 3-layer residual network as an example. X, Y : the data and label in the current batch; message STEP: begin training on the next batch; message TICK: sent from layer (process) i to layer (process) $i + 1$ after updating V_i ; message TOCK: sent from layer (process) $i + 1$ to layer (process) i after updating W_i ; message SYNC: after completing $n_updates$ updates on a batch, all processes synchronize with the main procedure and return results; message QUIT: training is complete, notify all processes to terminate.

The oscillating function below is fitted using a 5-layer network with sigmoid activation.

$$f(\mathbf{x}) = \begin{cases} x_1 x_2^2 \dots x_{d-1} x_d^2, & \mathbf{x} \in (-\infty, -1]^d; \\ x_1^2 x_2^2 \dots x_{d-1}^2 x_d^2, & \mathbf{x} \in (-\infty, -1]^d - (-\infty, -1]^d; \\ x_1^2 x_2 \dots x_{d-1}^2 x_d, & \mathbf{x} \in \{x_1 > 1, \dots, \text{or } x_d > 1\}. \end{cases}$$

As noted in Section VI-B, parallelization reduces the computation cost, albeit at the expense of additional communication overhead. In our experiments, the network width d predominantly governs the overall computation cost, since T_{mul} scales

super-linearly with d [43], while the communication cost remains nearly constant in a shared-memory configuration. Each test case was executed 5 times, and IV presents the mean runtime (in seconds) along with the corresponding standard deviations. The results indicate that when the network width

TABLE IV
PARALLEL VS. SERIAL RADMMs IN RUNTIME.

| d | Serial RADMM | Parallel RADMM |
|------|------------------------------|---------------------------------|
| 3000 | 253.8010 ± 1.0088 | 313.3090 ± 1.4582 |
| 4000 | 543.0684 ± 2.3043 | 603.5077 ± 1.5736 |
| 5000 | 1132.5736 ± 13.3211 | 1110.6362 ± 10.9119 |
| 5500 | 1650.6885 ± 24.2471 | 1551.2158 ± 107.8684 |
| 6000 | 2314.2873 ± 51.1496 | 1968.3845 ± 51.0245 |
| 6500 | 2711.8983 ± 19.6904 | 2483.0785 ± 59.7868 |

$d \geq 5000$, the runtime of the parallel implementation is lower than that of the serial implementation, as the computation cost becomes the dominant factor rather than communication overhead. Moreover, the performance advantage of the parallel implementation increases with the network dimension. These findings suggest that our parallel algorithm holds substantial potential for large-scale training problems.

VIII. CONCLUSION

In this paper, we propose both serial and parallel proximal (linearized) ADMM-based training algorithms for residual networks, leveraging a parallel regional update mechanism. We establish theoretical guarantees for convergence and demonstrate that our algorithms achieve an R-linear (or sublinear) convergence rate. Moreover, our analysis reveals that the parallel (distributed) RADMM algorithms offer advantages in terms of reduced time complexity and lower memory consumption. Additionally, we design and implement a control protocol for the parallel RADMMs using Python's multiprocessing and IPC. Experimental results demonstrate the fast and stable convergence, superior performance, and enhanced computational speed of our RADMM algorithms in training residual networks, further underscoring the benefits of the parallel implementation.

Potential extensions of this work include incorporating randomness into the data to design stochastic ADMMs, as well as developing and analyzing ADMM training algorithms for additional networks, such as CNNs and Transformers, to address image and natural language processing tasks. Finally, although our proof-of-concept implementation confirms the feasibility of our approach, the relatively high communication overhead in the parallel implementation partially offsets the benefits of parallelization, making the optimization of communication strategies a direction for future research.

IX. APPENDIX

A. Values of Parameters in Assumption 2

- $\underline{\beta}_i = \max \left\{ 32(1 + \sqrt{2})\mu(\psi_0\psi_2 + \psi_1^2 + \bar{\mathcal{V}}_i\psi_2 + \bar{\mathcal{V}}_{i-1}\psi_2), 16\mu\psi_1^2 \right\}$,
- $\underline{\beta}_N = 1$,

for some $\bar{\mathcal{V}}_0 \in (\|\mathbf{X}\|, +\infty)$ and $\{\bar{\mathcal{V}}_i\}_{i=1}^{N-1} \subseteq (0, +\infty)$,

- $\underline{\omega}_i := \frac{1}{16} \left(\frac{\beta_i}{4} - 8\mu(\psi_0\psi_2 + \psi_1^2 + \bar{\mathcal{V}}_i\psi_2 + \bar{\mathcal{V}}_{i-1}\psi_2) - \sqrt{\Delta_i} \right) + \hat{\epsilon}_i$,

where

$$\Delta_i := \left(\frac{\beta_i}{4} - 8\mu(\psi_0\psi_2 + \psi_1^2 + \bar{\psi}_i\psi_2 + \bar{\psi}_{i-1}\psi_2) \right)^2 - 128\mu^2(\psi_0\psi_2 + \psi_1^2 + \bar{\psi}_i\psi_2 + \bar{\psi}_{i-1}\psi_2)^2,$$

and $\hat{\epsilon}_i \in (0, \frac{\sqrt{\Delta_i}}{32})$, $i \in [N-1]$,

$$\bullet \bar{\omega}_i := \min \left\{ \frac{\frac{\beta_i}{4} - 8\mu(\psi_0\psi_2 + \psi_1^2 + \bar{\psi}_i\psi_2 + \bar{\psi}_{i-1}\psi_2) + \sqrt{\Delta_i}}{16} - \hat{\epsilon}_i, \sqrt{(\omega_i)^2 + \frac{\beta_i\omega_i}{16} - \frac{\beta_i\epsilon_i}{4}} \right\},$$

in which $\epsilon_i \in (0, \frac{\omega_i}{4})$, $i \in [N-1]$ with the $\{\bar{\psi}_i\}_{i=0}^{N-1}$.

B. Parallel Three-Splitting RADMM

Pseudocode of our parallel three-splitting RADMM training algorithm is shown in Algorithm 4.

Algorithm 4: Parallel Three-Splitting RADMMs

Input: \mathbf{X} , \mathbf{Y} , K , λ , μ , $\{\beta_i\}_{i=1}^N$, $\{\omega_i^k\}_{i=1}^{N-1}$, and $\{\mathbf{W}_i^0\}_{i=1}^N$.
 $\mathbf{V}_0^k \leftarrow \mathbf{X}$, $\mathbf{U}_i^0 \leftarrow \mathbf{W}_i^0 \mathbf{V}_{i-1}^0$, $\mathbf{V}_i^0 \leftarrow \mathbf{V}_{i-1}^0 + \sigma_i(\mathbf{U}_i^0)$,
 $i \in [N-1]$, $\mathbf{V}_N^0 \leftarrow \mathbf{W}_N^0 \mathbf{V}_{N-1}^0$ and $\mathbf{\Lambda}_i^0 \leftarrow \mathbf{0}$, $i \in [N]$.
parallel_for $i \in [N]$ **do**
 for $k \leftarrow 0$ to $K-1$ **do**
 if $i < N$ **then**
 | Update \mathbf{W}_i^{k+1} by iteration equation (19).
 else
 | Update \mathbf{W}_N^{k+1} by iteration equation (18).
 end
 if $i > 1$ **then** Retrieve necessary block variables from
 processor $i-1$;
 if $i < N$ **then**
 | Update \mathbf{U}_i^{k+1} by solving (20) in proximal ADMM
 (by iteration equation (21) in proximal linearized
 ADMM).
 end
 if $i < N$ **then** Retrieve necessary block variables from
 processor $i+1$;
 if $i < N-1$ **then**
 | Update \mathbf{V}_i^k by iteration equation (22).
 else if $i = N-1$ **then**
 | Update \mathbf{V}_{N-1}^{k+1} by iteration equation (23).
 else
 | Update \mathbf{V}_N^{k+1} by iteration equation (24).
 end
 if $i < N$ **then**
 | Update $\mathbf{\Lambda}_i^{k+1}$ by iteration equation (25).
 else
 | Update $\mathbf{\Lambda}_i^{k+1}$ by iteration equation (26).
 end
 end
end
Synchronize all processors.
Output: $\{\mathbf{W}_i^K\}_{i=1}^N$

C. Experimental Settings

Experiments in Section VII-A and Section VII-B are conducted on a laptop equipped with an Intel Core i5-11320H @ 3.20GHz CPU (4 cores 8 threads), and a server equipped with two Intel Xeon Gold 5218 @ 2.30GHz CPUs (16 cores 32 threads per socket), respectively. Parameters are initialized with a Kaiming normal distribution [44]. Training and testing data in Section VII-A are normalized as $\frac{x - x_{\min}}{x_{\max} - x_{\min}}$.

Parameters used in Section VII-A are listed as below, in which expansion factor EF_τ , EF_ι are multiplied to τ , ι after each epoch, respectively.

- Sigmoid. BP-based algorithms: learning rate = 0.01, weight decay = 0.0001, momentum = 0.9. 2SRADMM: $\text{EF}_\tau = 1.05$, $\text{EF}_\iota = 1.05$, $\beta = 10000$, $\mu = 0.1$, $\lambda = 0.05$ for $N \leq 10$, 5 for $10 < N \leq 30$, 50 otherwise, initial $\tau_i \equiv N$, $\iota_i \equiv N$. 3SRADMM: $\text{EF}_\tau = 1.05$, $\beta_i \equiv 1000$, $\mu = 0.1$, $\lambda = 0.0001$, initial $\tau_i \equiv 10$.

- ReLU. BP-based algorithms: SGD learning rate = $10^{-10}/\delta d$, SGD weight decay = $10^{-10}\delta d$, where $\delta = 10^{\lfloor 0.2N \rfloor}$, SGD momentum = 0.9, Adam learning rate = 0.01, adam weight decay = 1. 2SRADMM: $\text{EF}_\tau = 1.05$, $\text{EF}_\iota = 1.05$, $\beta = 10$, $\mu = 10^{-5}/dN$, $\lambda = 10^{-5}dN$, $\tau_i \equiv 10dN$, initial $\iota_i \equiv 10d$. 3SRADMM: $\text{EF}_\tau = 1.05$, $\beta_i \equiv 100$, $\mu = 1$, $\lambda = 0.0001$, initial $\tau_i \equiv 10$.

In addition, 10 samples $\{(\mathbf{x}_i, f(\mathbf{x}_i))\}_{i=1}^{10}$ are produced uniformly in $[-2, 2]$, and we take $\beta = 100$, $\mu = 0.1$, $\tau_i^k \equiv 1$, $\iota_i^k \equiv 1$, $\lambda = 0.005$ for $d = 3000, 4000$, and 0.001 for $d = 5000, 5500, 6000, 6500$ in the two-splitting proximal linearized RADMM in Section VII-B.

D. Proof of Proposition 1

We first define $\Theta_{\mathbf{X}_i^{k+1}}$ as $(\mathbf{X}_1^{k+1}, \dots, \mathbf{X}_{i-1}^{k+1}, \mathbf{X}_{i+1}^k, \dots, \mathbf{X}_n^k)$.

Proof: (Proof of Proposition 1) For the update of \mathbf{W}_N^k ,

$$\begin{aligned} \mathcal{L}_\beta^{2s}(\mathbf{W}_N^{k+1}; \Theta_{\mathbf{W}_N^{k+1}}) - \mathcal{L}_\beta^{2s}(\mathbf{W}_N^k; \Theta_{\mathbf{W}_N^k}) \\ = -\frac{\lambda}{2} \|\mathbf{W}_N^{k+1} - \mathbf{W}_N^k\|^2 - \frac{\beta}{2} \|(\mathbf{W}_N^{k+1} - \mathbf{W}_N^k)\mathbf{V}_{N-1}^k\|^2 \end{aligned}$$

by the first-order optimality condition of (8). For the update of each \mathbf{W}_i^k , $i \in [N-1]$, we have

$$\mathcal{L}_\beta^{2s}(\mathbf{W}_i^{k+1}; \Theta_{\mathbf{W}_i^{k+1}}) - \mathcal{L}_\beta^{2s}(\mathbf{W}_i^k; \Theta_{\mathbf{W}_i^k}) \leq -\frac{\omega_i^k}{2} \|\mathbf{W}_i^{k+1} - \mathbf{W}_i^k\|^2.$$

Similarly, we can estimate the change of \mathcal{L}_β^{2s} related to \mathbf{V}_i^k , $i \in [N-1]$. For the update of \mathbf{V}_N^k , we have

$$\mathcal{L}_\beta^{2s}(\mathbf{V}_N^{k+1}; \Theta_{\mathbf{V}_N^{k+1}}) - \mathcal{L}_\beta^{2s}(\mathbf{V}_N^k; \Theta_{\mathbf{V}_N^k}) \leq -\frac{1+\beta}{2} \|\mathbf{V}_N^{k+1} - \mathbf{V}_N^k\|^2$$

based on the strong convexity of the objective function of (14). For the update of $\mathbf{\Lambda}^k$, we have

$$\mathcal{L}_\beta^{2s}(\mathbf{\Lambda}^{k+1}; \Theta_{\mathbf{\Lambda}^{k+1}}) = \mathcal{L}_\beta^{2s}(\mathbf{\Lambda}^k; \Theta_{\mathbf{\Lambda}^k}) + \frac{1}{\beta} \|\mathbf{\Lambda}^{k+1} - \mathbf{\Lambda}^k\|^2.$$

Adding the above difference of adjacent iterations in the update of each block variable, we have

$$\begin{aligned} \mathcal{L}_\beta^{2s}(\Psi_{2s}^{k+1}) - \mathcal{L}_\beta^{2s}(\Psi_{2s}^k) \\ \leq -\frac{\lambda}{2} \|\mathbf{W}_N^{k+1} - \mathbf{W}_N^k\|^2 - \sum_{i=1}^{N-1} \frac{\omega_i}{2} \|\mathbf{W}_i^{k+1} - \mathbf{W}_i^k\|^2 \\ - \sum_{i=1}^{N-2} \frac{\nu_i}{2} \|\mathbf{V}_i^{k+1} - \mathbf{V}_i^k\|^2 - \frac{\mu}{2} \|\mathbf{V}_{N-1}^{k+1} - \mathbf{V}_{N-1}^k\|^2 \\ - \left(\frac{1+\beta}{4} - \frac{1}{2\beta} \right) (\|\mathbf{V}_N^{k+1} - \mathbf{V}_N^k\|^2 + \|\mathbf{\Lambda}^{k+1} - \mathbf{\Lambda}^k\|^2) \\ \leq -c_1 \|\Psi_{2s}^{k+1} - \Psi_{2s}^k\|^2, \end{aligned}$$

where $c_1 = \min\{\frac{\lambda}{2}, \{\frac{\omega_i^{\min}}{2}\}, \{\frac{\nu_i^{\min}}{2}\}, \mu, \frac{1+\beta}{4} - \frac{1}{2\beta}\} > 0$. \square

E. Proof of Proposition 2

First, upper boundness of $\{\|\mathbf{W}_i^k\|\}_{i=1}^N$, $\{\|\mathbf{V}_i^k\|\}_{i=1}^N$, $\{\|\mathbf{\Lambda}^k\|\}$ under Assumptions 1 is guaranteed in Lemma 2.

Lemma 2. There exist positive constants $\{\bar{\mathbf{W}}_i\}_{i=1}^N$, $\{\bar{\mathbf{V}}_i\}_{i=1}^N$, $\bar{\lambda}$ such that $\|\mathbf{W}_i^k\| \leq \bar{\mathbf{W}}_i$, $\|\mathbf{V}_i^k\| \leq \bar{\mathbf{V}}_i$, $i \in [N]$, $\|\mathbf{\Lambda}^k\| \leq \bar{\lambda}$.

Proof: By (15), we have

$$\begin{aligned} & \left(\frac{1}{2} - \frac{1}{2\beta} \right) \|\mathbf{V}_N^k - \mathbf{Y}\|^2 + \frac{\mu}{2} \sum_{i=1}^{N-1} \|\mathbf{V}_{i-1}^k + \sigma_i(\mathbf{W}_i^k \mathbf{V}_{i-1}^k) - \mathbf{V}_i^k\|^2 \\ & + \frac{\lambda}{2} \sum_{i=1}^N \|\mathbf{W}_i^k\|^2 + \frac{\beta}{2} \|\mathbf{W}_N^k \mathbf{V}_{N-1}^k - \mathbf{V}_N^k + \frac{1}{\beta} \boldsymbol{\Lambda}^k\|^2 < \infty \end{aligned}$$

by Proposition 1. If $\|\mathbf{W}_i^k\| \rightarrow \infty$, then $\mathcal{L}_\beta^{2s}(\Psi_{2s}^k) \rightarrow \infty$, a contradiction. Thus there exist $\bar{\mathcal{W}}_i > 0$ such that $\|\mathbf{W}_i^k\| \leq \bar{\mathcal{W}}_i$, $i \in [N]$. If $\|\mathbf{V}_N^k - \mathbf{Y}\|_F \rightarrow \infty$, then $\mathcal{L}_\beta^{2s}(\Psi_{2s}^k) \rightarrow \infty$, a contradiction. Thus there exist $\bar{\mathcal{V}}_N$ and $\bar{\lambda} > 0$ such that $\|\mathbf{V}_N^k\|_F \leq \bar{\mathcal{V}}_N$, $\|\boldsymbol{\Lambda}^k\|_F \leq \bar{\lambda}$. Similarly, the sequences $\{\|\mathbf{V}_i^k - \mathbf{V}_{i-1}^k\|_F\}$, $i \in [N-1]$ are also upper bounded. By $\mathbf{V}_0^k \equiv \mathbf{X}$, there exist $\bar{\mathcal{V}}_i > 0$ such that $\|\mathbf{V}_i^k\|_F \leq \bar{\mathcal{V}}_i$, $i \in [N-1]$. \square

Proof: (Proof of Proposition 2) By the first-order optimality condition of (8), we know that

$$\begin{aligned} \frac{\partial \mathcal{L}_\beta^{2s}}{\partial \mathbf{W}_N}(\Psi_{2s}^{k+1}) &= \beta \{ \mathbf{W}_N^{k+1} \mathbf{V}_{N-1}^{k+1} \mathbf{V}_{N-1}^{k+1 \top} - \mathbf{W}_N^{k+1} \mathbf{V}_{N-1}^k \mathbf{V}_{N-1}^{k \top} \\ &+ \mathbf{V}_N^k \mathbf{V}_{N-1}^{k \top} - \mathbf{V}_N^{k+1} \mathbf{V}_{N-1}^{k+1 \top} \} + \boldsymbol{\Lambda}^{k+1} \mathbf{V}_{N-1}^{k+1 \top} - \boldsymbol{\Lambda}^k \mathbf{V}_{N-1}^{k \top}. \end{aligned}$$

Thus we have

$$\begin{aligned} \left\| \frac{\partial \mathcal{L}_\beta^{2s}}{\partial \mathbf{W}_N}(\Psi_{2s}^{k+1}) \right\| &\leq \bar{\mathcal{V}}_{N-1} \|\boldsymbol{\Lambda}^{k+1} - \boldsymbol{\Lambda}^k\| + \beta \bar{\mathcal{V}}_{N-1} \|\mathbf{V}_N^{k+1} - \mathbf{V}_N^k\| \\ &+ (2\beta \bar{\mathcal{W}}_N \bar{\mathcal{V}}_{N-1} + \beta \bar{\mathcal{V}}_N + \bar{\lambda}) \|\mathbf{V}_{N-1}^{k+1} - \mathbf{V}_{N-1}^k\|. \end{aligned}$$

Similarly, we can estimate the norms of partial derivative of \mathcal{L}_β^{2s} with respect to \mathbf{W}_i , \mathbf{V}_i , and $\boldsymbol{\Lambda}$, respectively. Then

$$\begin{aligned} & \|\nabla \mathcal{L}_\beta^{2s}(\Psi_{2s}^{k+1})\| \\ & \leq \sum_{i=1}^N \left\| \frac{\partial \mathcal{L}_\beta^{2s}}{\partial \mathbf{W}_i}(\Psi_{2s}^{k+1}) \right\| + \sum_{i=1}^N \left\| \frac{\partial \mathcal{L}_\beta^{2s}}{\partial \mathbf{V}_i}(\Psi_{2s}^{k+1}) \right\| + \left\| \frac{\partial \mathcal{L}_\beta^{2s}}{\partial \boldsymbol{\Lambda}}(\Psi_{2s}^{k+1}) \right\| \\ & \leq \tilde{c} \left(\sum_{i=1}^N \|\mathbf{W}_i^{k+1} - \mathbf{W}_i^k\| + \sum_{i=1}^N \|\mathbf{V}_i^{k+1} - \mathbf{V}_i^k\| + \|\boldsymbol{\Lambda}^{k+1} - \boldsymbol{\Lambda}^k\| \right) \\ & \leq c_2 \|\Psi_{2s}^{k+1} - \Psi_{2s}^k\| \end{aligned}$$

for certain $\tilde{c} > 0$, and $c_2 := \sqrt{2N+1} \tilde{c} > 0$. \square

F. Proofs of Theorems 1 and 4

Proof: (Proof of Theorems 1 and 4) Based on Propositions 1 and 2, following from Theorem 2.9 of [45], Theorem 2 of [46] (Lemma 5 of [47]), and Theorem 1 of [24], we obtain the convergence results. \square

G. Proof of Lemma 1

Under the assumptions mentioned in Section V-B3, we first prove the sufficient descent of \mathcal{L}_R^{3s} and estimate the norm of gradient $\|\nabla \mathcal{L}_R^{3s}(\tilde{\Psi}_{3s}^k)\|$ as in Lemma 3 and Lemma 4.

Lemma 3. *The serial and parallel three-splitting RADMMS satisfy Proposition 1 with respect to \mathcal{L}_R^{3s} and $\tilde{\Psi}_{3s}$.*

Proof: Using the method similar to the proof of Proposition 1, we have

$$\begin{aligned} & \mathcal{L}_\beta^{3s}(\Psi_{3s}^{k+1}) + \sum_{i=1}^{N-1} \left(\frac{4(\omega_i)^2}{\beta_i} + \frac{\omega_i}{4} \right) \|\mathbf{U}_i^{k+1} - \mathbf{U}_i^k\|^2 \\ & + \sum_{i=1}^{N-1} (\tilde{\eta}_i + \frac{\mu}{4}) \|\mathbf{V}_i^{k+1} - \mathbf{V}_i^k\|^2 \\ & \leq \mathcal{L}_\beta^{3s}(\Psi_{3s}^k) + \sum_{i=1}^{N-1} \left(\frac{4(\omega_i)^2}{\beta_i} + \frac{\omega_i}{4} \right) \|\mathbf{U}_i^k - \mathbf{U}_i^{k-1}\|^2 \\ & + \sum_{i=1}^{N-1} (\tilde{\eta}_i + \frac{\mu}{4}) \|\mathbf{V}_i^k - \mathbf{V}_i^{k-1}\|^2 - \sum_{i=1}^{N-1} (\tilde{\eta}_i - \tilde{\eta}_i - \frac{\mu}{4}) \|\mathbf{V}_i^{k+1} - \mathbf{V}_i^k\|^2 \\ & - \sum_{i=1}^{N-1} (\hat{\theta}_i^{k+1} - \hat{\theta}_i^k - \frac{\omega_i^{k-1}}{4}) \|\mathbf{U}_i^{k+1} - \mathbf{U}_i^k\|^2 - \sum_{i=1}^{N-1} \frac{\mu}{4} \|\mathbf{V}_i^k - \mathbf{V}_i^{k-1}\|^2 \\ & - \sum_{i=1}^{N-1} \left(\frac{4(\omega_i)^2}{\beta_i} + \frac{\omega_i}{4} - \tilde{\theta}_i^k \right) \|\mathbf{U}_i^k - \mathbf{U}_i^{k-1}\|^2 \\ & - \frac{\lambda}{2} \sum_{i=1}^N \|\mathbf{W}_i^{k+1} - \mathbf{W}_i^k\|^2 - \left(\frac{1+\beta_N}{2} - \frac{1}{\beta_N} \right) \|\mathbf{V}_N^{k+1} - \mathbf{V}_N^k\|^2, \end{aligned}$$

where parameters

$$\begin{aligned} \hat{\theta}_i^{k+1} &:= \frac{\omega_i^k}{2} - \frac{4}{\beta_i} (\mu(\psi_0 \psi_2 + \psi_1^2 + (\bar{\mathcal{V}}_i + \bar{\mathcal{V}}_{i-1}) \psi_2) + \omega_i^k)^2, i \in [N-1]; \\ \hat{\eta}_i &:= \mu - \frac{4\mu^2 \psi_1^2}{\beta_{i+1}}, i \in [N-2], \quad \hat{\eta}_{N-1} := \frac{\mu}{2}; \\ \tilde{\theta}_i^k &:= \frac{4(\omega_i^{k-1})^2}{\beta_i}, i \in [N-1]; \\ \tilde{\eta}_i &:= \frac{4\mu^2 \psi_1^2}{\beta_i}, i \in [N-1]. \end{aligned}$$

It can be verified that $\frac{4(\omega_i)^2}{\beta_i} + \frac{\omega_i}{4} - \tilde{\theta}_i^k \geq \epsilon_i$, $\exists \kappa_i > 0$ such that $\hat{\theta}_i^{k+1} - \tilde{\theta}_i^k - \frac{\omega_i^{k-1}}{4} > \kappa_i$, $\hat{\eta}_i - \tilde{\eta}_i - \frac{\mu}{4} > 0$, $i \in [N-1]$, and $\frac{1+\beta_N}{2} - \frac{1}{\beta_N} > 0$.

Then, we have

$$\begin{aligned} & \mathcal{L}_\beta^{3s}(\Psi_{3s}^{k+1}) + \sum_{i=1}^{N-1} \theta_i \|\mathbf{U}_i^{k+1} - \mathbf{U}_i^k\|^2 + \sum_{i=1}^{N-1} \eta_i \|\mathbf{V}_i^{k+1} - \mathbf{V}_i^k\|^2 \\ & \leq \mathcal{L}_\beta^{3s}(\Psi_{3s}^k) + \sum_{i=1}^{N-1} \theta_i \|\mathbf{U}_i^k - \mathbf{U}_i^{k-1}\|^2 + \sum_{i=1}^{N-1} \eta_i \|\mathbf{V}_i^k - \mathbf{V}_i^{k-1}\|^2 \\ & - \sum_{i=1}^{N-1} \kappa_i \|\mathbf{U}_i^{k+1} - \mathbf{U}_i^k\|^2 - \sum_{i=1}^{N-1} (\hat{\eta}_i - \tilde{\eta}_i - \frac{\mu}{4}) \|\mathbf{V}_i^{k+1} - \mathbf{V}_i^k\|^2 \\ & - \sum_{i=1}^{N-1} \epsilon_i \|\mathbf{U}_i^k - \mathbf{U}_i^{k-1}\|^2 - \sum_{i=1}^{N-1} \frac{\mu}{4} \|\mathbf{V}_i^k - \mathbf{V}_i^{k-1}\|^2 \\ & - \frac{\lambda}{2} \sum_{i=1}^N \|\mathbf{W}_i^{k+1} - \mathbf{W}_i^k\|^2 - \left(\frac{1+\beta_N}{2} - \frac{1}{\beta_N} \right) \|\mathbf{V}_N^{k+1} - \mathbf{V}_N^k\|^2 \\ & \leq \mathcal{L}_\beta^{3s}(\Psi_{3s}^k) + \sum_{i=1}^{N-1} \theta_i \|\mathbf{U}_i^k - \mathbf{U}_i^{k-1}\|^2 + \sum_{i=1}^{N-1} \eta_i \|\mathbf{V}_i^k - \mathbf{V}_i^{k-1}\|^2 \\ & - \bar{c} \left(\sum_{i=1}^N \|\mathbf{W}_i^{k+1} - \mathbf{W}_i^k\|^2 + \sum_{i=1}^{N-1} \|\mathbf{U}_i^{k+1} - \mathbf{U}_i^k\|^2 \right. \\ & \left. + \sum_{i=1}^N \|\mathbf{V}_i^k - \mathbf{V}_i^{k-1}\|^2 + \sum_{i=1}^{N-1} \|\mathbf{U}_i^{k-1} - \mathbf{U}_i^{k-2}\|^2 \right. \\ & \left. + \sum_{i=1}^{N-1} \|\mathbf{V}_i^{k-1} - \mathbf{V}_i^{k-2}\|^2 \right), \end{aligned}$$

where $\bar{c} = \min\{\kappa_i, \bar{\eta}_i - \tilde{\eta}_i - \frac{\mu}{4}, \epsilon_i, \frac{\mu}{4}, \frac{\lambda}{2}, \frac{\beta_N^2 + \beta_N - 2}{2\beta_N}\} > 0$.

$$\begin{aligned} \sum_{i=1}^N \|\Lambda_i^{k+1} - \Lambda_i^k\|^2 &\leq \bar{c} \left(\sum_{i=1}^N (\|\mathbf{W}_i^{k+1} - \mathbf{W}_i^k\|^2 + \|\mathbf{V}_i^{k+1} - \mathbf{V}_i^k\|^2) \right. \\ &\quad \left. + \sum_{i=1}^{N-1} (\|\mathbf{U}_i^{k+1} - \mathbf{U}_i^k\|^2 + \|\mathbf{V}_i^k - \mathbf{V}_i^{k-1}\|^2 + \|\mathbf{U}_i^k - \mathbf{U}_i^{k-1}\|^2) \right) \end{aligned}$$

for certain $\tilde{c} > 0$. Therefore,

$$\begin{aligned} &\mathcal{L}_\beta^{3s}(\Psi_{3s}^{k+1}) + \sum_{i=1}^{N-1} \theta_i \|\mathbf{U}_i^{k+1} - \mathbf{U}_i^k\|^2 + \sum_{i=1}^{N-1} \eta_i \|\mathbf{V}_i^{k+1} - \mathbf{V}_i^k\|^2, \\ &\leq \mathcal{L}_\beta^{3s}(\Psi_{3s}^k) + \sum_{i=1}^{N-1} \theta_i \|\mathbf{U}_i^k - \mathbf{U}_i^{k-1}\|^2 + \sum_{i=1}^{N-1} \eta_i \|\mathbf{V}_i^k - \mathbf{V}_i^{k-1}\|^2 \\ &\quad - \frac{\bar{c}}{2} \left(\sum_{i=1}^N \|\mathbf{W}_i^{k+1} - \mathbf{W}_i^k\|^2 + \sum_{i=1}^{N-1} \|\mathbf{U}_i^{k+1} - \mathbf{U}_i^k\|^2 \right. \\ &\quad \left. + \sum_{i=1}^N \|\mathbf{V}_i^{k+1} - \mathbf{V}_i^k\|^2 + \sum_{i=1}^{N-1} \|\mathbf{U}_i^k - \mathbf{U}_i^{k-1}\|^2 \right. \\ &\quad \left. + \sum_{i=1}^{N-1} \|\mathbf{V}_i^k - \mathbf{V}_i^{k-1}\|^2 \right) - \frac{\bar{c}}{2\tilde{c}} \sum_{i=1}^N \|\Lambda_i^{k+1} - \Lambda_i^k\|^2 \\ &\leq \mathcal{L}_\beta^{3s}(\Psi_{3s}^k) + \sum_{i=1}^{N-1} \theta_i \|\mathbf{U}_i^k - \mathbf{U}_i^{k-1}\|^2 + \sum_{i=1}^{N-1} \eta_i \|\mathbf{V}_i^k - \mathbf{V}_i^{k-1}\|^2 \\ &\quad - \frac{\bar{c}}{2\tilde{c}} \left(\sum_{i=1}^N \|\mathbf{W}_i^{k+1} - \mathbf{W}_i^k\|^2 + \sum_{i=1}^{N-1} \|\mathbf{U}_i^{k+1} - \mathbf{U}_i^k\|^2 \right. \\ &\quad \left. + \sum_{i=1}^N \|\mathbf{V}_i^{k+1} - \mathbf{V}_i^k\|^2 + \sum_{i=1}^N \|\Lambda_i^{k+1} - \Lambda_i^k\|^2 \right. \\ &\quad \left. + \sum_{i=1}^{N-1} \|\mathbf{U}_i^k - \mathbf{U}_i^{k-1}\|^2 + \sum_{i=1}^{N-1} \|\mathbf{V}_i^k - \mathbf{V}_i^{k-1}\|^2 \right), \end{aligned}$$

which means $\mathcal{L}_R^{3s}(\tilde{\Psi}_{3s}^{k+1}) \leq \mathcal{L}_R^{3s}(\tilde{\Psi}_{3s}^k) - \frac{\bar{c}}{2\tilde{c}} \|\tilde{\Psi}_{3s}^{k+1} - \tilde{\Psi}_{3s}^k\|^2$. \square

Lemma 4. *The serial and parallel three-splitting RADMMs satisfy Proposition 2 with respect to \mathcal{L}_R^{3s} and $\tilde{\Psi}_{3s}$.*

In order to prove Lemma 4, we first estimate the boundness lemma in Lemma 5.

Lemma 5. *There exist positive constants $\bar{\mathcal{V}}_N$, $\{\bar{\lambda}_i\}_{i=1}^N$, $\{\bar{\mathcal{W}}_i\}_{i=1}^N$, and $\{\bar{\mathcal{U}}_i\}_{i=1}^{N-1}$ such that $\|\mathbf{V}_N^k\| \leq \bar{\mathcal{V}}_N$, $\|\Lambda_i^k\| \leq \bar{\lambda}_i$, $\|\mathbf{W}_i^k\| \leq \bar{\mathcal{W}}_i$, $i \in [N]$, $\|\mathbf{U}_i^k\| \leq \bar{\mathcal{U}}_i$, $i \in [N-1]$.*

Proof: Noting that for each $i \in [N-1]$,

$$\|\Lambda_i^k\|^2 \leq 2\mu^2 \psi_1^2 (\sqrt{nd}\psi_0 + \bar{\mathcal{V}}_{i-1} + \bar{\mathcal{V}}_i)^2 + 2(\omega_i^{k-1})^2 \|\mathbf{U}_i^k - \mathbf{U}_i^{k-1}\|^2,$$

then $\mathcal{I}^k - \sum_{i=1}^{N-1} \frac{\mu^2 \psi_1^2}{\beta_i} (\sqrt{nd}\psi_0 + \bar{\mathcal{V}}_{i-1} + \bar{\mathcal{V}}_i)^2 \leq \mathcal{L}_R^{3s}(\tilde{\Psi}_{3s}^k)$, in which

$$\begin{aligned} \mathcal{I}^k &:= \left(\frac{1}{2} - \frac{1}{2\beta_N} \right) \|\mathbf{V}_N^k - \mathbf{Y}\|^2 + \frac{\lambda}{2} \sum_{i=1}^N \|\mathbf{W}_i^k\|^2 \\ &\quad + \frac{\mu}{2} \sum_{i=1}^{N-1} \|\mathbf{V}_{i-1}^k + \sigma_i(\mathbf{U}_i^k) - \mathbf{V}_i^k\|^2 + \sum_{i=1}^{N-1} \eta_i \|\mathbf{V}_i^k - \mathbf{V}_i^{k-1}\|^2 \\ &\quad + \sum_{i=1}^{N-1} \frac{\beta_i}{2} \|\mathbf{W}_i^k \mathbf{V}_{i-1}^k - \mathbf{U}_i^k + \frac{1}{\beta_i} \Lambda_i^k\|^2 \\ &\quad + \frac{\beta_N}{2} \|\mathbf{W}_N^k \mathbf{V}_{N-1}^k - \mathbf{V}_N^k + \frac{1}{\beta_N} \Lambda_N^k\|^2 \\ &\quad + \sum_{i=1}^{N-1} \left(\theta_i - \frac{(\omega_i^{k-1})^2}{\beta_i} \right) \|\mathbf{U}_i^k - \mathbf{U}_i^{k-1}\|^2. \end{aligned}$$

It can be verified that $\theta_i - \frac{(\omega_i^{k-1})^2}{\beta_i} \geq \frac{3(\omega_i)^2}{\beta_i} + \frac{3\omega_i}{16} + \frac{\epsilon_i}{4} > 0$, $i \in [N-1]$. By Lemma 4, $\{\mathcal{L}_R^{3s}(\tilde{\Psi}_{3s}^k)\}$ is upper bounded. If $\|\mathbf{V}_N^k\| \rightarrow \infty$, then $\mathcal{L}_R^{3s}(\tilde{\Psi}_{3s}^k) \rightarrow \infty$, a contradiction. Thus there exists $\mathcal{V}_N > 0$ such that $\|\mathbf{V}_N^k\| \leq \bar{\mathcal{V}}_N$. By $\Lambda_N^k = \mathbf{V}_N^k - \mathbf{Y}$, there exists $\bar{\lambda}_N > 0$ such that $\|\Lambda_N^k\| \leq \bar{\lambda}_N$. If $\|\mathbf{U}_i^k - \mathbf{U}_i^{k-1}\| \rightarrow \infty$, then $\mathcal{L}_R^{3s}(\tilde{\Psi}_{3s}^k) \rightarrow \infty$, a contradiction. Thus there exist $\chi_i > 0$ such that $\|\mathbf{U}_i^k - \mathbf{U}_i^{k-1}\| \leq \chi_i$, $i \in [N-1]$. According to $\Lambda_i^k = \mu(\mathbf{V}_{i-1}^k + \sigma_i(\mathbf{U}_i^{k-1}) - \mathbf{V}_i^{k-1}) \odot \sigma_i'(\mathbf{U}_i^{k-1}) + \tau_i^{k-1}(\mathbf{U}_i^k - \mathbf{U}_i^{k-1})$, there exist $\bar{\lambda}_i > 0$ such that $\|\Lambda_i^k\| \leq \bar{\lambda}_i$, $i \in [N-1]$. If $\|\mathbf{W}_i^k\| \rightarrow \infty$, then $\mathcal{L}_R^{3s}(\tilde{\Psi}_{3s}^k) \rightarrow \infty$, a contradiction. Thus there exist $\bar{\mathcal{W}}_i > 0$ such that $\|\mathbf{W}_i^k\| \leq \bar{\mathcal{W}}_i$, $i \in [N]$. By the following inequality:

$$\begin{aligned} &\sum_{i=1}^{N-1} \frac{\beta_i}{2} \|\mathbf{W}_i^k \mathbf{V}_{i-1}^k - \mathbf{U}_i^k + \frac{1}{\beta_i} \Lambda_i^k\|^2 \\ &\geq \sum_{i=1}^{N-1} \frac{\beta_i}{2} (\|\mathbf{U}_i^k\| - \bar{\mathcal{W}}_i \bar{\mathcal{V}}_{i-1} - \frac{1}{\beta_i} \bar{\lambda}_i)^2 \end{aligned}$$

for sufficiently large $\|\mathbf{U}_i^k\|$. If $\|\mathbf{U}_i^k\| \rightarrow \infty$, then $\mathcal{L}(\tilde{\Psi}_{3s}^k) \rightarrow \infty$, a contradiction. Thus there exists $\bar{\mathcal{U}}_i > 0$ such that $\|\mathbf{U}_i^k\| \leq \bar{\mathcal{U}}_i$, $i \in [N-1]$. \square

Proof: (Proof of Lemma 4) With similar arguments as in the proof of Proposition 2, we have

$$\begin{aligned} &\|\nabla \mathcal{L}_\beta^{3s}(\Psi_{3s}^{k+1})\| \\ &\leq \sum_{i=1}^N \left\| \frac{\partial \mathcal{L}_\beta^{3s}}{\partial \mathbf{W}_i}(\Psi_{3s}^{k+1}) \right\| + \sum_{i=1}^N \left\| \frac{\partial \mathcal{L}_\beta^{3s}}{\partial \mathbf{V}_i}(\Psi_{3s}^{k+1}) \right\| \\ &\quad + \sum_{i=1}^{N-1} \left\| \frac{\partial \mathcal{L}_\beta^{3s}}{\partial \mathbf{U}_i}(\Psi_{3s}^{k+1}) \right\| + \sum_{i=1}^N \left\| \frac{\partial \mathcal{L}_\beta^{3s}}{\partial \Lambda_i}(\Psi_{3s}^{k+1}) \right\| \\ &\leq \hat{c} \left(\sum_{i=1}^N (\|\mathbf{W}_i^{k+1} - \mathbf{W}_i^k\| + \|\mathbf{V}_i^{k+1} - \mathbf{V}_i^k\| + \|\Lambda_i^{k+1} - \Lambda_i^k\|) \right. \\ &\quad \left. + \sum_{i=1}^{N-1} (\|\mathbf{U}_i^{k+1} - \mathbf{U}_i^k\| + \|\mathbf{V}_i^k - \mathbf{V}_i^{k-1}\| + \|\mathbf{U}_i^k - \mathbf{U}_i^{k-1}\|) \right) \end{aligned}$$

for certain $\hat{c} > 0$. Thus

$$\begin{aligned} &\|\nabla \mathcal{L}(\tilde{\Psi}_{3s}^{k+1})\| \\ &\leq \|\nabla \mathcal{L}_\beta^{3s}(\Psi_{3s}^{k+1})\| + 4 \sum_{i=1}^{N-1} (\theta_i \|\mathbf{U}_i^{k+1} - \mathbf{U}_i^k\| + \eta_i \|\mathbf{V}_i^{k+1} - \mathbf{V}_i^k\|) \\ &\leq c_2 \|\tilde{\Psi}_{3s}^{k+1} - \tilde{\Psi}_{3s}^k\|, \end{aligned}$$

where $c_2 = \sqrt{6N-3}(\hat{c} + 4 \max\{\{\theta_i\}_{i=1}^{N-1}, \{\eta_i\}_{i=1}^{N-1}\})$. \square

Proof: (Proof of Lemma 1) By Lemmas 3 and 4, with similar arguments as in the proof of Theorems 1 and 4, we obtain the results. \square

H. Proofs of Theorems 3 and 4

Proof: (Proof of Theorems 3 and 4) We only need to establish the connections between $\{\mathcal{L}_\beta^{3s}, \Psi_{3s}\}$ and $\{\mathcal{L}_R^{3s}, \tilde{\Psi}_{3s}\}$. For the iteration point sequence,

$$\begin{aligned} &\tilde{\Psi}_{3s}^k - \tilde{\Psi}_{3s}^* \\ &= (\Psi_{3s}^k - \Psi_{3s}^*, \text{vec}(\mathbf{U}_i)^{k-1} - \text{vec}(\mathbf{U}_i)^*, \text{vec}(\mathbf{V}_i)^{k-1} - \text{vec}(\mathbf{V}_i)^*). \end{aligned}$$

Then we have $\|\Psi_{3s}^k - \Psi_{3s}^*\|^2 \leq \|\tilde{\Psi}_{3s}^k - \tilde{\Psi}_{3s}^*\|^2$. Moreover,

$$\begin{aligned}\mathcal{L}_\beta^{3s}(\Psi_{3s}^*) &= \lim_{k \rightarrow \infty} \mathcal{L}_\beta^{3s}(\Psi_{3s}^k) + \lim_{k \rightarrow \infty} \sum_{i=1}^{N-1} \theta_i \|U_i^k - U_i^{k-1}\|^2 \\ &+ \lim_{k \rightarrow \infty} \sum_{i=1}^{N-1} \eta_i \|V_i^k - V_i^{k-1}\|^2 = \mathcal{L}_R^{3s}(\tilde{\Psi}_{3s}^*).\end{aligned}$$

Thus $\mathcal{L}_\beta^{3s}(\Psi_{3s}^k) - \mathcal{L}_\beta^{3s}(\Psi_{3s}^*) \leq \mathcal{L}_R^{3s}(\tilde{\Psi}_{3s}^k) - \mathcal{L}_R^{3s}(\tilde{\Psi}_{3s}^*)$. \square

X. ACKNOWLEDGMENTS

The authors would like to thank Yau Mathematical Sciences Center, Tsinghua University for providing the computing resources to support our research. We thank Dr. Xixi Jia for helpful suggestions.

REFERENCES

- [1] K. He, X. Zhang, S. Ren, and J. Sun, "Deep residual learning for image recognition," in *Proc. IEEE Conf. Comput. Vis. Pattern Recognit.*, pp. 770–778, 2016.
- [2] A. Vaswani, N. Shazeer, N. Parmar, J. Uszkoreit, L. Jones, A. N. Gomez, Ł. Kaiser, and I. Polosukhin, "Attention is all you need," in *Proc. Adv. Neural Inf. Process. Syst.*, vol. 30, 2017.
- [3] J. Devlin, M.-W. Chang, K. Lee, and K. Toutanova, "BERT: pre-training of deep bidirectional transformers for language understanding," 2018, *arXiv: 1810.04805*.
- [4] T. B. Brown, B. Mann, N. Ryder, M. Subbiah, J. Kaplan, P. Dhariwal, A. Neelakantan, P. Shyam, G. Sastry, A. Askell, S. Agarwal, A. Herbert-Voss, G. Krueger, T. Henighan, R. Child, A. Ramesh, D. M. Ziegler, J. Wu, C. Winter, C. Hesse, M. Chen, E. Sigler, M. Litwin, S. Gray, B. Chess, J. Clark, C. Berner, S. McCandlish, A. Radford, I. Sutskever, and D. Amodei, "Language models are few-shot learners," in *Proc. Adv. Neural Inf. Process. Syst.*, vol. 33, pp. 1877–1901, 2020.
- [5] OpenAI, "GPT-4 technical report," 2023, *arXiv:2303.08774*.
- [6] G. Taylor, R. Burmeister, Z. Xu, B. Singh, A. Patel, and T. Goldstein, "Training neural networks without gradients: a scalable ADMM approach," in *Proc. 33rd Int. Conf. Mach. Learn.*, vol. 48, pp. 2722–2731, 2016.
- [7] Z. Allen-Zhu, Y. Li, and Z. Song, "A convergence theory for deep learning via over-parameterization," in *Proc. 36th Int. Conf. Mach. Learn.*, vol. 97, pp. 242–252, 2019.
- [8] Y. Cui, Z. He, and J.-S. Pang, "Multicomposite nonconvex optimization for training deep neural networks," *SIAM J. Optim.*, vol. 30, no. 2, pp. 1693–1723, 2020.
- [9] J. de Jesús Rubio, "Stability analysis of the modified Levenberg-Marquardt algorithm for the artificial neural network training," *IEEE Trans. Neural Netw. Learn. Syst.*, vol. 32, no. 8, pp. 3510–3524, 2021.
- [10] J. Zeng, S.-B. Lin, Y. Yao, and D.-X. Zhou, "On ADMM in deep learning: convergence and saturation-avoidance," *J. Mach. Learn. Res.*, vol. 22, no. 199, pp. 1–67, 2021.
- [11] J. Li, M. Xiao, C. Fang, Y. Dai, C. Xu, and Z. Lin, "Training neural networks by lifted proximal operator machines," *IEEE Trans. Pattern Anal. Mach. Intell.*, vol. 44, no. 6, pp. 3334–3348, 2022.
- [12] W. Liu, X. Liu, and X. Chen, "Linearly constrained nonsmooth optimization for training autoencoders," *SIAM J. Optim.*, vol. 32, no. 3, pp. 1931–1957, 2022.
- [13] J. Wang, H. Li, Z. Chai, Y. Wang, Y. Cheng, and L. Zhao, "Toward quantized model parallelism for graph-augmented MLPs based on gradient-free ADMM framework," *IEEE Trans. Neural Netw. Learn. Syst.*, vol. 35, no. 4, pp. 4491–4501, 2024.
- [14] D. P. Kingma and J. L. Ba, "Adam: A method for stochastic optimization," 2017, *arXiv: 1412.6980*.
- [15] A. Choromanska, B. Cowen, S. Kumaravel, R. Luss, M. Rigotti, I. Rish, B. Kingsbury, P. DiAchille, V. Gurev, R. Tejwani, and D. Bounoufouf, "Beyond backprop: Online alternating minimization with auxiliary variables," in *Proc. 36th Int. Conf. Mach. Learn.*, vol. 97, pp. 1193–1202, 2019.
- [16] F. Gu, A. Askari, and L. E. Ghaoui, "Fenchel lifted networks: A Lagrange relaxation of neural network training," in *Proc. Int. Conf. Artif. Intell. Statist.*, vol. 108, pp. 3362–3371, 2020.
- [17] I. Goodfellow, Y. Bengio, and A. Courville, *Deep Learning*. MIT Press, 2016.
- [18] M. Á. Carreira-Perpiñán and W. Wang, "Distributed optimization of deeply nested systems," in *Proceedings of the Seventeenth International Conference on Artificial Intelligence and Statistics*, vol. 33, pp. 10–19, 2014.
- [19] D.-R. Han, "A survey on some recent developments of alternating direction method of multipliers," *J. Oper. Res. Soc. China*, vol. 10, pp. 1–52, 2022.
- [20] J. Zeng, T. T.-K. Lau, S.-B. Lin, and Y. Yao, "Global convergence of block coordinate descent in deep learning," in *Proc. 36th Int. Conf. Mach. Learn.*, vol. 97, pp. 7313–7323, 2019.
- [21] J. Wang, F. Yu, X. Chen, and L. Zhao, "ADMM for efficient deep learning with global convergence," in *Proc. ACM SIGKDD Int. Conf. Knowl. Discovery Data Mining*, p. 111–119, 2019.
- [22] J. Wang, Z. Chai, Y. Cheng, and L. Zhao, "Toward model parallelism for deep neural network based on gradient-free ADMM framework," in *Proc. IEEE Int. Conf. Data Min.*, pp. 591–600, 2020.
- [23] W. Liu, X. Liu, and X. Chen, "An inexact augmented Lagrangian algorithm for training leaky ReLU neural network with group sparsity," *J. Mach. Learn. Res.*, vol. 24, no. 212, pp. 1–43, 2023.
- [24] J. Xu, C. Bao, and W. Xing, "Convergence rates of training deep neural networks via alternating minimization methods," *Optim. Lett.*, vol. 18, pp. 909–923, 2024.
- [25] X. Lai, J. Cao, X. Huang, T. Wang, and Z. Lin, "A maximally split and relaxed ADMM for regularized extreme learning machines," *IEEE Trans. Neural Netw. Learn. Syst.*, vol. 31, no. 6, pp. 1899–1913, 2020.
- [26] L. Deng, Y. Wu, Y. Hu, L. Liang, G. Li, X. Hu, Y. Ding, P. Li, and Y. Xie, "Comprehensive SNN compression using ADMM optimization and activity regularization," *IEEE Trans. Neural Netw. Learn. Syst.*, vol. 34, no. 6, pp. 2791–2805, 2023.
- [27] M. Fazel, T. K. Pong, D. Sun, and P. Tseng, "Hankel matrix rank minimization with applications to system identification and realization," *SIAM Journal on Matrix Analysis and Applications*, vol. 34, no. 3, pp. 946–977, 2013.
- [28] X. Li, D. Sun, and K.-C. Toh, "A Schur complement based semiproximal ADMM for convex quadratic conic programming and extensions," *Math. Program.*, vol. 155, pp. 333–373, 2016.
- [29] M. Hong and Z.-Q. Luo, "On the linear convergence of the alternating direction method of multipliers," *Math. Program.*, vol. 162, pp. 165–199, 2017.
- [30] L. Yang, T. K. Pong, and X. Chen, "Alternating direction method of multipliers for a class of nonconvex and nonsmooth problems with applications to background/foreground extraction," *SIAM J. Imaging Sci.*, vol. 10, no. 1, pp. 74–110, 2017.
- [31] Y. Wang, W. Yin, and J. Zeng, "Global convergence of ADMM in nonconvex nonsmooth optimization," *J. Sci. Comput.*, vol. 78, pp. 29–63, 2019.
- [32] A. Harlap, D. Narayanan, A. Phanishayee, V. Seshadri, N. Devanur, G. Ganger, and P. Gibbons, "PipeDream: Fast and efficient pipeline parallel DNN training," 2018, *arXiv:1806.03377*.
- [33] H. Lee, C.-J. Hsieh, and J.-S. Lee, "Local critic training for model-parallel learning of deep neural networks," *IEEE Trans. Neural Netw. Learn. Syst.*, vol. 33, no. 9, pp. 4424–4436, 2022.
- [34] D. P. Bertsekas, *Convex Optimization Algorithms*. Athena Scientific, 2015.
- [35] K. Kurdyka, "On gradients of functions definable in o-minimal structures," *Ann. Inst. Fourier*, vol. 48, no. 3, pp. 769–783, 1998.
- [36] S. Łojasiewicz, "Une propriété topologique des sous-ensembles analytiques réels," in *Les Équations aux Dérivées Partielles*, pp. 87–89, Paris: Éditions du Centre National de la Recherche Scientifique, 1963.
- [37] S. Łojasiewicz, "Sur la géométrie semi- et sous-analytique," *Ann. Inst. Fourier*, vol. 43, no. 5, pp. 1575–1595, 1993.
- [38] B. S. Mordukhovich, *Variational Analysis and Generalized Differentiation I: Basic Theory*. Berlin, Heidelberg: Springer-Verlag, 2006.
- [39] R. T. Rockafellar and R. J.-B. Wets, *Variational Analysis*. Springer-Verlag, 1998.
- [40] H. Attouch, J. Bolte, P. Redont, and A. Soubeyran, "Proximal alternating minimization and projection methods for nonconvex problems: an approach based on the Kurdyka-Łojasiewicz inequality," *Math. Oper. Res.*, vol. 35, no. 2, pp. 438–457, 2010.
- [41] G. Li and T. K. Pong, "Calculus of the exponent of Kurdyka-Łojasiewicz inequality and its applications to linear convergence of first-order methods," *Found. Comput. Math.*, vol. 18, pp. 1199–1232, 2018.
- [42] S. G. Krantz and H. R. Parks, *A Primer of Real Analytic Functions*. 2002.
- [43] V. V. Williams, Y. Xu, Z. Xu, and R. Zhou, "New bounds for matrix multiplication: from alpha to omega," in *Proceedings of the 2024 Annual ACM-SIAM Symposium on Discrete Algorithms*, 2024.

- [44] K. He, X. Zhang, S. Ren, and J. Sun, "Delving deep into rectifiers: Surpassing human-level performance on ImageNet classification," in *Proceedings of the IEEE International Conference on Computer Vision (ICCV)*, 2015.
- [45] H. Attouch, J. Bolte, and B. F. Svaiter, "Convergence of descent methods for semi-algebraic and tame problems: proximal algorithms, forward-backward splitting, and regularized Gauss-Seidel methods," *Math. Program.*, vol. 137, pp. 91–129, 2013.
- [46] H. Attouch and J. Bolte, "On the convergence of the proximal algorithm for nonsmooth functions involving analytic features," *Math. Program.*, vol. 116, pp. 5–16, 2009.
- [47] P. Baque, J.-H. Hours, F. Fleuret, and P. Fua, "A provably convergent alternating minimization method for mean field inference," 2015, *arXiv:1502.05832*.